Selenate Reduction by Granular Iron and the Associated Isotope Fractionation

by

Heather Kayleigh Shrimpton

A thesis

presented to the University of Waterloo

in fulfillment of the

thesis requirement for the degree of

Master of Science

in

Earth Sciences

Waterloo, Ontario, Canada, 2013

Author's Declaration

I hereby declare that I am the sole author of this thesis. This is a true copy of the thesis, including any required final revisions, as accepted by my examiners.

I understand that my thesis may be made electronically available to the public.

Abstract

Research in selenium isotopes has been gaining interest as new contaminated sites are identified around the world. Selenium is an emerging contaminant, as it is increasingly being released through anthropogenic activities. It is an element with a very narrow range between nutrient requirement and toxic concentrations. Increased concentrations in the environment are a cause for concern. Selenium can be made less toxic in a system through reduction.

Currently, investigations into fractionation caused by the reduction of Se by Fe and Fe minerals are limited. This thesis describes a batch study conducted using granular iron to treat Se(VI) in $CaCO_3$ saturated water, under anaerobic conditions. The amount of Se(VI) in solution decreased to 14.5% of the initial concentration within three days. No quantifiable Se(IV) was found in solution. Analysis of the solid phase showed Se(IV), ferric selenite, FeSe, and Se(0) on the GI. The mass of Se^0 on the GI increased over time. Iron selenide compounds became more prevalent after two days had elapsed. Effective fractionations of 4.3‰ for $^{82/76}Se$ and 3.0‰ for $^{82/78}Se$ were observed for this reaction. These effective fractionations are lower than fractionations observed in other experiments for reduction in solution. This discrepancy may be due to the reduction of Se(IV) occurring after adsorbing onto the solid phase, rather than reduction taking place only in solution.

Acknowledgements

I thank my supervisor, Dr. David Blowes, for his enthusiastic technical assistance whenever lab work hit a snag. I would also like to thank Dr. Carol Ptacek, for advice on surprise precipitates during method development, and Richard Amos, for his technical experience with flow meters.

I am grateful for funding provided by an NSERC Discovery Grant awarded to D.W. Blowes and an Ontario Research Fund - Re grant awarded to D.W. Blowes, C.J. Ptacek and R.T. Amos.

Aspects of this research were performed at GeoSoilEnviroCARS (Sector 13), Advanced Photon Source (APS), Argonne National Laboratory. GeoSoilEnviroCARS is supported by the National Science Foundation - Earth Sciences (EAR-0622171) and Department of Energy - Geosciences (DE-FG02-94ER14466). Use of the Advanced Photon Source was supported by the U.S. Department of Energy, Office of Science, Office of Basic Energy Sciences, under Contract No. DE-AC02-06CH11357.

A huge thanks goes to Laura Groza for being a font of knowledge. Thanks also go to Joy Hu for help in the lab. Immense thanks go to Blair Gibson and Julia Jamieson-Hanes for the lengthy isotope discussions and invaluable knowledge about both the Neptune and method development. Thanks also to Romy Matthies for useful isotope talks and the sharing of equipment. Jing Ma provided company in the lab for odd work hours. Jeffery Sparks, for knowing where to find anything and everything in the lab. Jeff Bain, for general assistance. I should also thank my family and my friends, for their support throughout this entire process.

Dedication

For my family, the fish, and the baby ducks.

Table of Contents

List of Figures ..... **vii**

List of Tables ..... **viii**

List of Abbreviations ..... **ix**

Chapter 1: *Introduction* **1**
- **1.1 Background** **2**
  - 1.1.1 Se in the environment 2
  - 1.1.2 Removal of Se from groundwater 5
  - 1.1.3 Se isotope measurements 7
  - 1.1.4 Se isotope fractionation 9
- **1.2 Research Objectives** **12**
- **1.3 Thesis Organization** **13**

Chapter 2: *Fractionation of Selenium During Selenate Reduction by Granular Iron in a Calcite-Saturated Solution* **14**
- **2.1 Chapter Summary** **14**
- **2.2 Introduction** **14**
- **2.3 Methods** **16**
  - 2.3.1 Experimental method 16
  - 2.3.2 Geochemical analysis 18
  - 2.3.3 Solid phase data collection 18
  - 2.3.4 Isotope sample preparation 19
  - 2.3.5 Isotope measurements 19
- **2.4 Results** **20**
  - 2.4.1 Geochemical analysis 20
  - 2.4.2 Solid sample analysis 22
  - 2.4.3 Isotope results 29
- **2.5 Discussion** **31**
  - 2.5.1 Geochemistry 31
    - 2.5.1.1 Alkalinity, calcium, pH and Eh 31
    - 2.5.1.2 Selenium concentrations and speciation 33
    - 2.5.1.3 Modeling of geochemical data 34
  - 2.5.2 The solid phase 35
  - 2.5.3 Isotopes 36
- **2.6 Summary** **37**

Chapter 3: *Conclusions* **39**

Chapter 4: *Recommendations for Future Research* **41**

References **44**

Appendix **52**

List of Figures

Figure 1.1: pe-pH diagram for Se at STP, with an Se activity of 10^{-6} mol/L, after Séby et al. 2001. 4
Figure 1.2: The pH dependent adsorption of Se(IV) on calcite, where total Se is 1.9 x 10^{-2} mmol/L from Goldberg and Glaubig (1988). Circles represent experimental data. 7
Figure 2.1: The variation in a few of the geochemical parameters over the length of the experiment: a) pH, b) alkalinity, and concentrations in solution of c) selenium and d) calcium. Error bars on selenium concentration measurements were smaller than the symbols, so were not included. 21
Figure 2.2: XANES scans from selected samples along the batch experiment time line. Standards used to determine the valence states composing each sample are on the bottom. Arrow points to lack of peak on 15 min sample 23
Figure 2.3: Non-normalized XANES scans from selected samples along the batch experiment time line. The difference in absorbance is related to the quantity of Se on the solid sample. 24
Figure 2.4: Linear combination fittings using Se(0), Se(IV), Se(VI), $FeSe_2$, FeSe, and $Fe_2(SeO_3)_3$, as well as the difference between the data and the best fit, for the 48 hr and 72 hr XANES samples. 26
Figure 2.5: Linear combination fittings using Se(0), Se(IV), Se(VI), $FeSe_2$, FeSe, and $Fe_2(SeO_3)_3$, as well as the difference between the data and the best fit, for the 21 hr and 36 hr XANES samples. 27
Figure 2.6: Linear combination fittings using Se(0), Se(IV), Se(VI), $FeSe_2$, FeSe, and $Fe_2(SeO_3)_3$, as well as the difference between the data and the best fit, for the 48 hr and 72 hr XANES samples. 28
Figure 2.7: Se isotope results for the fractionation of Se(VI) by granular iron. a) The $\delta 82/78$Se values, and b) the $\delta 82/76$ values. Error bars represent the external reproducibility of the NIST SRM3149 (2σ), while the first error bar is the external reproducibility of the stock solution (2σ). Arrows in both diagrams point to the batch samples that were selected for XANES analysis. 30

List of Tables

Table 1: A few of the relevant elements and dimers that interfere with the measurement of Se isotopes. 8
Table 2.1: XANES fit from the program ATHENA for Se batch experiment using GI. No Se(VI) was found on any of the samples. 25
Table 2.2: Saturation indexes of important phases. Results are from modeling experimental data using PHREEQCI. 35

List of Abbreviations

DI	deionized
GI	granular iron
GSE-CARS	GeoSoilEnviro-Center for Advanced Radiation Sources
HG–MC–ICP–MS	hydride generation coupled to multi-collector inductively coupled mass spectrometry
ICP–OES	inductively coupled plasma optical emission spectrometry
ICP–MS	inductively coupled plasma mass spectrometry
NIST	National Institute of Standards and Technology
PRB	permeable reactive barrier
SPE	solid phase extraction
SRM	standard reference material
TCF	thiol cotton fiber
TIMS	thermal-ionization mass spectrometry
XANES	X-ray absorption near edge structure

Chapter 1:

Introduction

The element selenium is a trace nutrient, typically existing in low concentrations in the environment (Lemly 2004). However, some areas have higher concentrations that can produce a range of health defects in both humans and wildlife (Winkel et al. 2012). Selenium occurs in five common oxidation states, Se(VI), Se (IV) Se(0), Se (-1) and Se(-II). Of these oxidation states, Se(VI) is of the greatest concern because Se(VI) is ten times as toxic as Se(IV) (USA EPA 1996), whereas Se(0), Se(-I), and Se(-II) are less soluble. As a result, reduction is the most favorable method of treatment (Ellis et al. 2003; Martens and Suarez 1997). Although there has been some difficulty measuring Se isotope fractionation in the sediment of water bodies (Clark and Johnson 2008; Clark and Johnson 2010; Johnson 2012), fractionation from reduction in anoxic groundwater systems should be discernible. *In situ* reduction could be enhanced by the introduction of a material such as granular iron (GI). If total Se concentration, solid phase, and speciation analysis are also performed, a tool for estimating the removal of Se from groundwater due to reduction by GI can be developed. The main goal of this thesis was to determine the isotope fractionation caused by the reduction of Se(VI) by GI in $CaCO_3$ saturated water, without the obfuscation of transport. This chapter gives some background on how Se enters the environment, how it migrates, a few of the *in situ* removal methods, and current isotope research. It also contains a brief overview of the methods required to measure Se isotopes.

1.1 Background

1.1.1 Se in the environment

There are several regions in the world where Se is an element of concern, as it has reached levels that affect the health of wildlife and may pose a severe risk to humans. The Kesterson Reservoir, which became contaminated due to agricultural run-off and evaporation, had Se concentrations measured in the hundreds of parts-per-billion (White et al. 1991). More recently, studies on groundwater moving through or past the weathered Mancos shale in the Southern United States have recorded concentrations of Se on the scale of mg/L (Morrison et al. 2012). Whereas some countries, such as China and India, have extremely variable quantities of Se in the soil, it can range up to several hundred ppm in shale (Lenz and Lens 2009; Wen and Carignan 2011).

Localized enrichment of Se is sometimes due to the native geology, but it is often anthropogenic activities, such as mining, smelting, coal burning, and agriculture, that release this element into the environment at concentrations sufficiently high to cause concern (Lenz and Lens 2009). Aquatic wildlife are especially sensitive due to bioaccumulation (Lemly 2004), although it is still ambiguous whether biomagnification of Se occurs (Van Dyke et al. 2013). Bioaccumulation in Sturgeon in the San Francisco Bay area could lead to toxic levels of Se, despite concentrations of less than 1 μg/L Se in the water, for instance (Young et al. 2010).

Consequences of increasing Se concentrations can be sudden; it only takes a rise from the ng/L range to 10 μg/L in water to cause complete reproductive failure

in sensitive fish species (Lemly 2002). Certain toad species experienced not only a decrease in the survival rate of embryos, but also developmental abnormalities in 55-58% of the remaining clutch at Se levels of up to 100 μg/g dry mass (Hopkins et al. 2005). The typical result of increased Se concentrations is usually reproductive impairment or teratogenicity, but has also resulted in the deaths of livestock (Van Dyke et al. 2013; Plant et al. 2003). In humans, exceeding the recommended limit of 400 μg/day of Se can cause nail and hair loss, liver damage, digestive system problems, disruption of the nervous system, and certain types of cancer (Plant et al. 2003). Regular intake of Se above 75 μg/day, which is still within the recommended limit, can increase the risk of diabetes (Winkel et al. 2012). Se can be immobilized via reduction, a process that may be more readily identified in groundwater systems by examining the Se isotope ratios, rather than observed changes in concentration along a flow path that could be due to other factors. It may be vital to ensure Se is removed in groundwater before that groundwater discharges into an open water body, creating potentially avoidable tragedy.

Selenium has five oxidation states: Se(VI), as selenate (SeO_4^{2-}); Se(IV), as selenite (SeO_3^{2-}) or hydroselenite ($HSeO_3^-$); Se(0), or elemental Se; Se(-I); and Se(-II) (Figure 1.1). The varied oxidation states make it possible to use selenium stable isotopes to trace reduction processes in some natural systems (Rouxel et al. 2002).

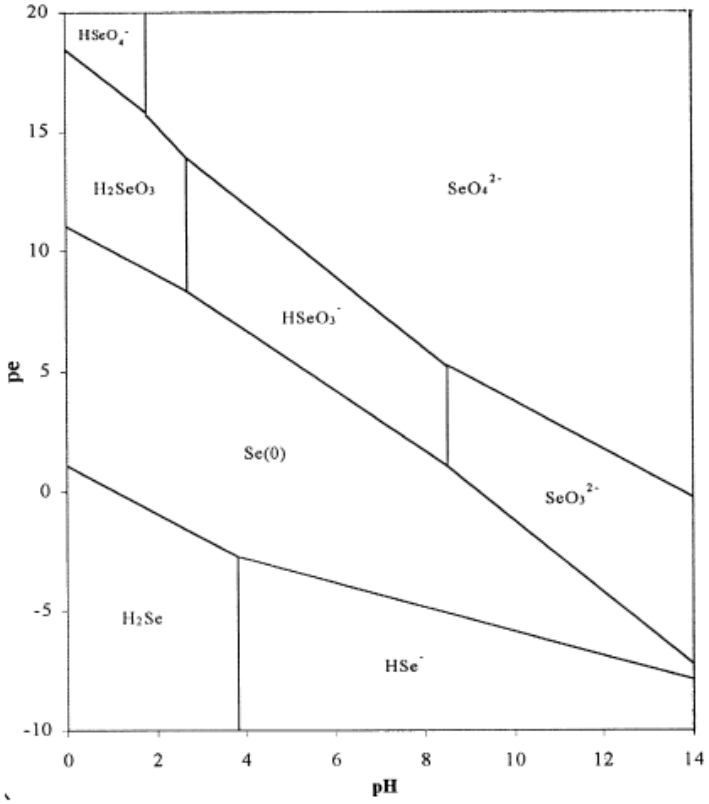

Figure 1.1: pe-pH diagram for Se at STP, with an Se activity of 10^{-6} mol/L, after Séby et al. 2001.

The oxidized valence states (Se (VI) and Se (IV)) are the most mobile forms of Se, as both are highly soluble. They pose the highest contamination threat. Selenite is less mobile as it has a greater propensity to adsorb onto sediment, even at near-neutral pH (Schilling et al. 2011b; Torres et al. 2010). However, though Se(IV) is less toxic, it is more bioavailable than Se(VI) (Schilling et al. 2011a; USA EPA 1996). Both biotic and abiotic reactions can reduce Se(VI) to Se(IV) as it travels through the subsurface (Johnson 2004). Under favorable conditions, Se(IV) can be further reduced to either Se(0) or Se(-II). Selenides are typically found bound in metal selenides, organo-selenides, or $H_2Se_{(g)}$, depending on the pH (Elrashidi et al. 1987). Metal selenides are reasonably insoluble, and tend to be stable, while organo-selenides are less toxic, and $H_2Se_{(g)}$ is volatile, so can leave the system. Elemental Se

is stable under most anoxic conditions (Figure 1.1), so transformation from the oxidized species to Se(0) or Se(-II) is considered a method of removing Se (Ellis et al. 2003; Martens and Suarez 1997; Peters et al. 1999; White et al. 1991).

1.1.2 Removal of Se from groundwater

Research into techniques for Se removal from natural waters has been gathering interest over the years as new occurrences of high concentrations are discovered (Lemly 2004; Winkel et al. 2012). Researchers have typically focused on sorption to soil, clays, and Fe minerals as a removal mechanism, as these materials are often already present in the environment (Boult et al. 1998; Dhillon and Dhillon 1999; Goh and Lim 2004; Hayes et al. 1987; Kim et al. 2012; Mondal et al. 2004; Rovira et al. 2008). Soil and clay alone are generally found to not sorb SeO_4^{2-}, and were inefficient at adsorbing $HSeO_3^-$ and SeO_3^{2-} at pH of 7 and higher (Neal et al. 1987a). The ability of fungi, algae, and bacteria to volatilize Se has been examined, but is usually more applicable in shallow ground or open water environments (Amouroux and Donard 1997; Herbel et al. 2000; Schilling et al. 2013).

The necessary groundwater chemistry for precipitation or reduction to occur has also been investigated, but precipitation is usually dependent on the composition of the aquifer (Basu et al. 2007; Kent et al. 1994; Mondal et al. 2004). Typically, groundwater systems become anoxic either because of isolation from the atmosphere due to depth or confinement, or high concentrations of organic carbon or other nutrients that allowed aerobic bacteria to consume the oxygen. In these groundwater systems, the more permanent method of Se removal is through

reduction, as Se(0) is stable under anoxic conditions (Breynaert et al. 2010; Martens and Suarez 1997).

Iron minerals and GI have proven effective in the reduction of Se(VI) and Se(IV) (Gibson et al. 2012; Loyo et al. 2008; Mondal et al. 2004; Morrison et al. 2002; Sasaki et al. 2008b). Green rust and pyrite have also been found to be successful at Se removal, but may not exist naturally or be stable under all conditions (Johnson and Bullen 2003; Mitchell et al. 2013). GI can be used in permeable reactive barriers (PRB) to remove Se(VI) and Se(IV) from groundwater via reduction (Blowes et al. 2000; Sasaki et al. 2008b). However, reduction of Se by Fe is slow due to diffusion constraints of the solution into the GI (Ellis et al. 2003; Johnson et al. 1999). The reduction of water by iron also produces alkaline conditions. Sorption of Se(IV) and Se(VI) is lower at higher pH (Peak and Sparks 2002; Zhang and Sparks 1990).

The presence of Ca increases Se(IV) sorption with increased pH (Chakraborty et al. 2010; Goldberg and Glaubig 1988; Neal et al. 1987a). Groundwater is often supersaturated with respect to calcium carbonate ($CaCO_3$), so it is likely to precipitate along the flow path, especially at higher pH. Ca alone will not reduce Se(IV), but Se(IV) adsorbed to Ca can be reduced by Fe (Aurelio et al. 2010; Chakraborty et al. 2010; Goldberg and Glaubig 1988). The fractionation of Se isotopes has yet to be investigated for such a system.

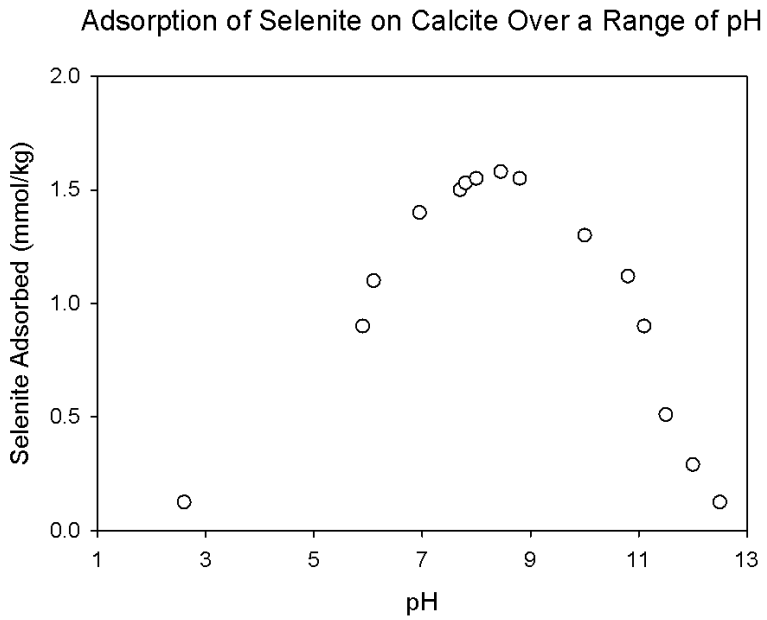

Figure 1.2: The pH dependent adsorption of Se(IV) on calcite, where total Se is 1.9 x 10^{-2} mmol/L from Goldberg and Glaubig (1988)**. Circles represent experimental data.**

1.1.3 Se isotope measurements

Selenium has six stable isotopes: 74 (0.89%), 76 (9.37%), 77 (7.63%), 78 (23.77%), 80 (49.61%), and 82 (8.73%) (De Laeter et al. 2003). The measurement of Se isotopes by MC-ICP-MS has been historically difficult due to many spectral interferences, including that of Ar itself (Table 1). Although larger degrees of fractionation were measurable using conventional techniques (Krouse and Thode 1962; Rashid and Krouse 1985; Rees and Thode 1966), better tools were required to reduce error, and minimize the quantity of Se necessary to perform measurements. Multiple mathematical corrections were and are still required to remove the effects of spectral interferences (Goossens et al. 1994). These corrections are difficult to perform without adequate blank measurements and a sufficient number of Faraday cups to simultaneously collect signals of potentially interfering species.

Table 1: A few of the relevant elements and dimers that interfere with the measurement of Se isotopes.

Isotope	Interferences
74	$^{58}Ni^{16}O^+$, $^{37}Cl_2^+$, ^{74}Ge, $^{40}Ar^{34}S^+$,
76	$^{60}Ni^{16}O^+$, $^{36}Ar^{40}Ar^+$, $^{38}Ar_2^+$, $^{75}AsH^+$, ^{76}Ge,
77	$^{61}Ni^{16}O^+$, $^{40}Ar^{37}Cl^+$, $^{76}SeH^+$,
78	$^{62}Ni^{16}O^+$, $^{38}Ar^{40}Ar^+$, ^{78}Kr, $^{77}SeH^+$,
80	$^{40}Ar_2^+$, ^{80}Kr, $^{32}S^{16}O_3^+$,
82	$^{40}Ar_2H_2^+$, ^{82}Kr, $^{34}S^{16}O_3^+$, $^{81}BrH^+$

Thermal ionization mass spectrometry (TIMS) is used to eliminate the Ar interferences (Johnson et al. 1999), but there are limitations on the number of isotopes that can be measured simultaneously, as well as the effects of instrumental fractionation. A double spike is used to solve the latter problem with reasonable success (Johnson 2012). A multi-collector inductively coupled plasma mass spectrometer (MC-ICP-MS) coupled with a collision cell can be employed to reduce the interference from the Ar dimers (Rouxel et al. 2002; Rouxel et al. 2000). A standard sample bracketing method, which partially addressed issues with instrumental fractionation, is sometimes used, but collision cells using hydrogen gas cause another source of interference due to selenium hydrides.

Despite difficulties caused by hydrides, the in-line use of a hydride generator was found to reduce certain other interferences while boosting the signal intensities so that lower quantities of Se are needed for analysis (Elwaer and Hintelmann 2007; Rouxel et al. 2002). Interferences caused by hydrides can be removed mathematically, provided there are enough available Faraday cups (Clark and Johnson 2010; Elwaer and Hintelmann 2008a). Alternatively, a hydride generator

can be used offline during the sample preparation process to avoid the creation of hydrides and some plasma instability, at the cost of signal intensities (Ellis et al. 2003; Herbel et al. 2002; Herbel et al. 2000).

The use of MC-ICP-MS required modification of the previously convenient $\delta^{80/76}$Se ratio and 82/74 spike method for TIMS measurements (Johnson et al. 1999), because the intensity of the Ar dimer swamps the signal of ^{80}Se, and ^{82}Se is the most convenient replacement. Most current studies report the $^{82/76}$Se ratio (Clark and Johnson 2010; Layton-Matthews et al. 2006; Mitchell et al. 2012; Schilling et al. 2013), and some studies determine, but do not necessarily report, the $^{82/78}$Se ratio (Elwaer and Hintelmann 2008a; Mitchell et al. 2013); although this ratio is impinged on by $^{77}SeH^+$, it has a much smaller Ar dimer interference. Less interference from Ar could result in overall lower error.

Selenium isotope ratios are presented using delta notation, which is calculated using the following formula:

$$\delta^{\frac{82}{76}}Se = \left[\frac{(^{82}Se/^{76}Se)_{sample}}{(^{82}Se/^{76}Se)_{standard}} - 1\right] \times 1000‰ \quad (1.1)$$

where the standard is the NIST SRM 3149 (Carignan and Wen 2007), which has roughly the same isotopic composition as bulk earth.

1.1.4 Se isotope fractionation

Selenium isotope fractionation is observed during reactions where the reaction rates differ for the differing isotopes. Reduction of Se species is one example of a reaction path that results in measurable isotope fractionation (Johnson and Bullen 2004). In general, heavier isotopes remain in the higher valence state,

while the lower valence states become enriched in the lighter isotopes (Johnson 2012). If the reduced product is removed from the system during the progress of the reaction, the solution will become enriched in the heavier isotope and the $\delta^{82}Se$ values for the solution will become more positive as the reaction progresses. Meanwhile, any solid phase that selenium has adsorbed to or precipitated on would be depleted in the heavier isotopes and will have more negative $\delta^{82}Se$ values throughout the reaction. The fractionation factor, α, and the effective fractionation, ε, are defined as follows:

(1.2) $$\alpha_{A-B} = \frac{Ratio_A}{Ratio_B}$$

where A is the reactant, and B is the product.

(1.3) $$\varepsilon_{A-B} = (\alpha_{A-B} - 1) \times 1000‰$$

which is roughly equivalent to:

(1.4) $$\varepsilon_{A-B} \approx \delta_{reactant} - \delta_{product}$$

where the effective fractionation is positive when the product is enriched in lighter isotopes (Johnson and Bullen 2004; Mitchell et al. 2013). Note that not all of the literature on Se isotopes defines ε in this manner, so it is best to look at the context of the study before assuming the direction of fractionation. A comprehensive list of effective fractionations due to the reduction of Se can be found in Johnson (2012).

Ellis et al. (2003) observed relatively high fractionation of Se during reduction in batch and column experiments. Herbel et al. (2000) saw much lower fractionation using pure microbial cultures. Clark and Johnson (2008, 2010) examined the fractionation in the water, sediment, and plants of a wetland

environment to see if they could find a link between observed fractionation and reduction, but unfortunately, actual fractionation factors caused by plants in wetland environments were much lower than originally measured in laboratories (Johnson 2004). Fractionation in sediment occurs mostly in a narrow portion of the uppermost layer, slowly increasing with depth over time (Clark and Johnson 2010). Attempting to measure the Se fractionation in these sediments leads to an averaging effect, so using Se fractionation to monitor remediation in wetland sediment may not be feasible over short time periods (Johnson 2012). However, investigating Se fractionation in groundwater to determine whether reduction can be observed still has potential, as groundwater flow rates are often faster than diffusion, and the systems are of a much larger scale.

Selenium isotopes are also variable enough in nature that they are considered a valid biological tracer for fish, whose absorption of Se from the environment does not cause significant fractionation (Clark and Johnson, 2010). The provenance of yeast can also be determined using Se isotopes (Far et al., 2010). Selenium isotopes can thus be used to track any organism that does not significantly fractionate the element when consumed (Johnson 2012).

1.2 Research Objectives

The primary objective of the research detailed in this thesis is to add to the knowledge of Se(VI) fractionation through reduction. Isotope analysis could be used to determine the mechanism of removal in environments where direct observation is not necessarily possible, such as in groundwater flow systems. When combined with solid phase analysis and concentration measurements from laboratory studies, the feasibility of using Se isotopes for such an endeavor can be investigated. Selenium cycling is geochemically complicated, and work on Se isotopes currently remains limited. Topics covered by this particular thesis include:

- Measuring fractionation of Se isotopes due to reduction by GI
- Verifying the mechanism of removal by analyzing the solid phase, looking at the relative abundances of Se species

1.3 Thesis Organization

This thesis is presented as a research paper related to the objectives outlined in the previous section. The paper, given as Chapter 2, details the results of a batch experiment using a calcium carbonate saturated solution and GI to treat Se(VI). The solid phase, aqueous concentrations, and isotope ratios are all examined. Chapter 3 gives a summary of findings as they relate to the broader world of the study of Se isotopes. The final chapter contains recommendations for future research. Details about how the specific method used to measure Se isotopes differs from others, and the data reduction procedure, are found in the appendix.

Chapter 2:

Fractionation of Selenium During Selenate Reduction by Granular Iron in a Calcite-Saturated Solution

2.1 Chapter Summary

A batch experiment using granular iron and calcium carbonate saturated water was conducted to assess the treatment of Se(VI) under anaerobic conditions that are characteristic of many aquifers. Only 14.5% of the Se(VI) remained in solution after three days. Isotope measurements were made using HG-MC-ICP-MS (Neptune, Thermo Scientific). The fractionation factor associated with this reaction was 4.3‰ for $^{82/76}$Se. XANES analysis confirmed the presence of Se(0), Se(IV), and iron selenide on the solid phase.

2.2 Introduction

Selenium has one of the narrowest ranges between essential nutrient and harmfulness among the elements (Fernández-Martínez and Charlet 2009). An uptake greater than 400 μg/day can be toxic (Levander and Burk 2006). Normally, Se concentrations in the environment are quite low, in the ng/L range for water and 0.4 mg/kg for soils, on average (Plant et al. 2003). Selenium can be released into the environment as a product of agriculture, mining, smelting, and coal-burning industries, as well as through the natural weathering of Se-rich geological deposits, like some black shales (Lemly 2004; Wen and Carignan 2011; Winkel et al. 2012). These processes can lead to Se concentrations in groundwater as high as 4.7 mg/L (Morrison et al. 2012), while guidelines have a limit of 50 μg/L in the USA and 10

μg/L in Canada (Plant et al. 2003). Selenium concentrations in soil have been found as high as 5,000 mg/kg (Plant et al. 2003), and some coal deposits in China have Se concentrations of up to 6,500 mg/kg (Plant et al. 2003).

Selenium occurs in five common oxidation states: selenate, Se(VI); selenite, Se(IV); native selenium, Se(0); and the selenide forms Se(-I) and Se(-II). Selenate does not adsorb effectively under most conditions (Neal et al. 1987a). Selenite will adsorb weakly to clays, and more effectively to Fe minerals (Scheinost et al. 2008) and Ca minerals (Goldberg and Glaubig 1988), so reduction is a preferable solution for the elimination of Se. Once adsorbed, Se(IV) could be further reduced to elemental Se or metal selenides, states that are both more stable and immobile (Loyo et al. 2008; Martens and Suarez 1997; Scheinost et al. 2008).

Iron has been used in the past to treat Se-rich groundwater (Morrison et al. 2002), and has been tested in the laboratory under both flow and batch conditions in granular form (Gibson et al. 2012; Qiu et al. 2000; Sasaki et al. 2008b). However, the fractionation of Se isotopes associated with this material has yet to be investigated. Iron can directly reduce Se(VI) in the following reaction:

(2.1) $$SeO_4^{2-} + Fe_{(s)} + H_2O \rightarrow SeO_3^{2-} + Fe^{2+} + 2OH^-$$

Examining the concentration and speciation of Se alone may not be sufficient to determine whether it is successfully being treated in a groundwater setting, where sampling procedures can cause dilution, and sample storage procedures can alter speciation (Conde and Sanz Alaejos 1997). If the effective fractionation and the associated mechanism can be discerned, it will be possible to deduce whether granular iron (GI) is effectively treating Se in groundwater.

Many groundwater systems are saturated with respect to Ca due to the presence of limestone, dolomite, and the abundance of carbonate minerals in unconsolidated sediments. The reduction of water in GI PRBs release H_2 gas and OH^-, causing an increase in pH:

(2.2) $$Fe^0 + 2H_2O \rightarrow Fe^{2+} + H_{2(g)} + 2OH^-$$

The increase in pH causes the dissociation of bicarbonate and favors the precipitation of $CaCO_3$. As a result, carbonate minerals are likely to accumulate with GI in the path of groundwater flow (Chakraborty et al. 2010). The presence of Ca in the system could enhance the removal of selenium from groundwater due to co-precipitation, as Se(IV) (SeO_3^{2-}) is structurally similar to carbonate (CO_3^{2-}) (Fernández-Martínez and Charlet 2009). Calcium has also been found to increase the pH at which Se(IV) most effectively adsorbs, increasing the rate of Se(IV) removal under more alkaline conditions (Goldberg and Glaubig 1988; Neal et al. 1987b).

2.3 Methods

2.3.1 Experimental method

A batch test was conducted to determine the fractionation factor associated with the anaerobic reduction of Se(VI) by $CaCO_3$ weathered GI. The method used was similar to that of Jamieson-Hanes et al. (2012).

Prior to the initiation of the experiments, the GI was prepared by sieving Fe grains to obtain particles between 0.25 – 1.19 mm (16 to 60 mesh). Any oxides on the GI surface were then removed by immersing it in 1 M HCl, stirring and replacing the solution as the reactivity decreased, until the GI was uniformly black. The GI was

then packed into a column in an anaerobic chamber, and $CaCO_3$ saturated Ar purged water was pumped through it for two weeks. After reducing conditions had been established, the column was disassembled, and the GI was placed in an amber bottle stored under anaerobic conditions.

The experiment was conducted in an anaerobic chamber (Coy Laboratory Products Inc., Grass Lake, MI) to better approximate anoxic groundwater conditions. Calcium carbonate saturated water was prepared by adding sufficient $CaCO_3$ per liter of MilliQ DI water to supersaturate the solution, then dissolving it by bubbling the solution with $CO_{2(g)}$. A stock solution was prepared by adding $NaSeO_4$ (Sigma Aldrich) to a concentration of 10.33 mg/L (7.23×10^{-5} molal) Se(VI) as SeO_4^{2-}. The solution was then purged with Ar gas to remove O_2 and excess CO_2. To initiate the experiment, 100 mL of the 10.33 mg/L Se solution was dispensed into 250 mL glass amber bottles containing 5.00 ± 0.09 g of prepared GI.

The contents of each bottle were sacrificed in duplicate over a three day period. In order to establish a time series with a higher initial density of sample points, not all of the shorter time period bottles were initiated on the same day. The reaction between the GI and Se was recorded as having ended when the sample was filtered using a vacuum filtration apparatus with qualitative coarse filter paper to remove the GI. The GI was then collected for later analysis.

The pH, Eh, and alkalinity were measured on unfiltered portions of each set of bottles in the time series. Alkalinity measurements used bromocresol green-methyl red indicator and a digital titrator (Hach Co., USA) with a 0.16 N H_2SO_4 cartridge. Filtered samples were also taken for cations, anions, speciation, and

isotopes, using 0.2 μm filters (Acrodisc, Pall, UK) and polyethylene syringes (BD, Franklin Lakes, NJ). Only the cation samples were acidified using concentrated HNO_3 (Omnitrace ultra, EMD Millipore). The GI samples were maintained under anaerobic conditions until they could be freeze-dried.

2.3.2 Geochemical analysis

Cation samples were analyzed for major cations, such as Fe and Ca, using inductively coupled plasma-optical emission spectrometry (ICP-OES; Thermo Scientific ICAP 6500). Speciation analysis for Se(VI) and Se(IV) was performed using a Dionex IC 5000 with a Dionex IonPac AS18 2x 250 mm column and IonPac AG18 2x50 mm guard column. This system could analyze samples with Se concentrations as low as 1 mg/L. To verify the speciation analysis, the total Se concentration in solution according to ICP-OES minus the determined Se(VI) concentration using IC was compared to the measured value of Se(IV) using IC.

2.3.3 Solid phase data collection

Iron samples were prepared for XANES analysis by packing the freeze-dried samples in an Al sample holder covered in kapton tape in an anaerobic glove box, following the same method as Jamieson-Hanes et al. (2012). Samples were analyzed at GSE-CARS beamline 13-BM-D at the Advanced Photon Source (APS; Argonne, IL, USA). Aluminum foil was placed over the detector during measurement to reduce the background signal from the GI. Standards measured at this time included elemental Se, Na_2SeO_4, and Na_2SeO_3. Additional FeSe, $Fe_2(SeO_3)_3$, and $FeSe_2$ standards were later obtained from the Actinide Reference X-ray Absorption Spectroscopy database (AcXAS) (Charlet et al. 2007; Missana et al. 2009; Scheinost

et al. 2013; Scheinost et al. 2008; Scheinost and Charlet 2008). The resulting XANES data were processed using the program ATHENA (Ravel and Newville 2005).

2.3.4 Isotope sample preparation

Isotope samples were spiked before purification using an approximately 1:1 mix of ^{74}Se and ^{77}Se, so that there was roughly twice as much ^{77}Se as ^{78}Se in the final sample (Elwaer and Hintelmann 2008a; Mitchell et al. 2012; Schilling et al. 2011a; Zhu et al. 2008). Sufficient concentrated ultra pure HCl (Lab distilled trace metal grade HCl, Fisher Scientific) was added to achieve a concentration of 8 mol/L. The samples were allowed to reduce over night before diluting to 1 mol/L HCl. After 30 minutes, the samples were purified with thiol cotton fiber (TCF), prepared using the method of Rouxel et al. (2002). A mass of 0.1 g of TCF was loaded onto 1 mL polyethylene SPE columns, prior to applying the separation method (Layton-Matthews et al. 2006). The procedure followed the extraction steps of Elwaer and Hintelmann (2008b).

The final reduction step after purification resulted in 15 mL samples with a Se concentration of 80 μg/L, and an HCl concentration of 2 mol/L. Due to the potential presence of interfering elements introduced by the TCF, blanks for isotope analysis were run through the same sample purification process. Samples were allowed to sit over night before analysis (Schilling and Wilcke 2010).

2.3.5 Isotope measurements

Isotope analyses were conducted using hydride generation coupled to a multi collector inductively coupled plasma mass spectrometer. (HG-MC-ICP-MS), with a similar method to Elwaer and Hintelmann (2008) and Schilling et al. (2011). A LI-2

hydride generation system was connected to the MC-ICP-MS (Thermo Instruments Neptune) to boost the signal intensities. A 0.4% $NaBH_4$, 0.2% NaOH solution provided the $H_{2(g)}$ source. A magnetic stirrer was used to help disperse bubbles in the $NaBH_4$ solution, increasing stability. Samples and standards were pre-mixed with acid, which increased signal stability.

Standards (NIST SRM3149) were run after every fourth sample. After rinsing with 4N HCl until Se is below detection, blanks were run between every sample. For $^{82/78}$Se, an internal precision of 0.04‰ (2σ, N=4) on the NIST SRM3149, and an external precision of 0.17‰ (2σ, N=24) was maintained. For $^{82/76}$Se, the internal precision was 0.06‰, and the external precision was 0.52‰. Delta values for each sample were calculated using the closest standard.

Data reduction, including interference correction methods, was performed using an iterative procedure (Siebert et al. 2001). Krypton was not found to be a significant interference in our gas source, and Br was also not found to be a significant interference.

2.4 Results

2.4.1 Geochemical analysis

Calcium concentrations temporarily increased to higher than initial stock solution values, before gradually decreasing over time (Figure 2.1). The maximum Ca concentrations occurred after 30 minutes had elapsed. Total alkalinity (as $CaCO_3$) decreased at about the same rate as the Ca concentration (Figure 2.1).

Dissolved Fe concentrations were below the quantifiable limit of 0.7 mg/L for all samples. After about 21 hrs had lapsed, there was some Fe above the detection limit of 0.2 mg/L.

The pH at the start of the batch tests was higher than at the end (Figure 2.1). The first pH measured at 30 min was the lowest, and the last batch flask to be filled (15 min) had the highest pH. There was a small calibration problem for the pH probe when the measurement was taken for the 60 hr sample, resulting in a lower value for pH.

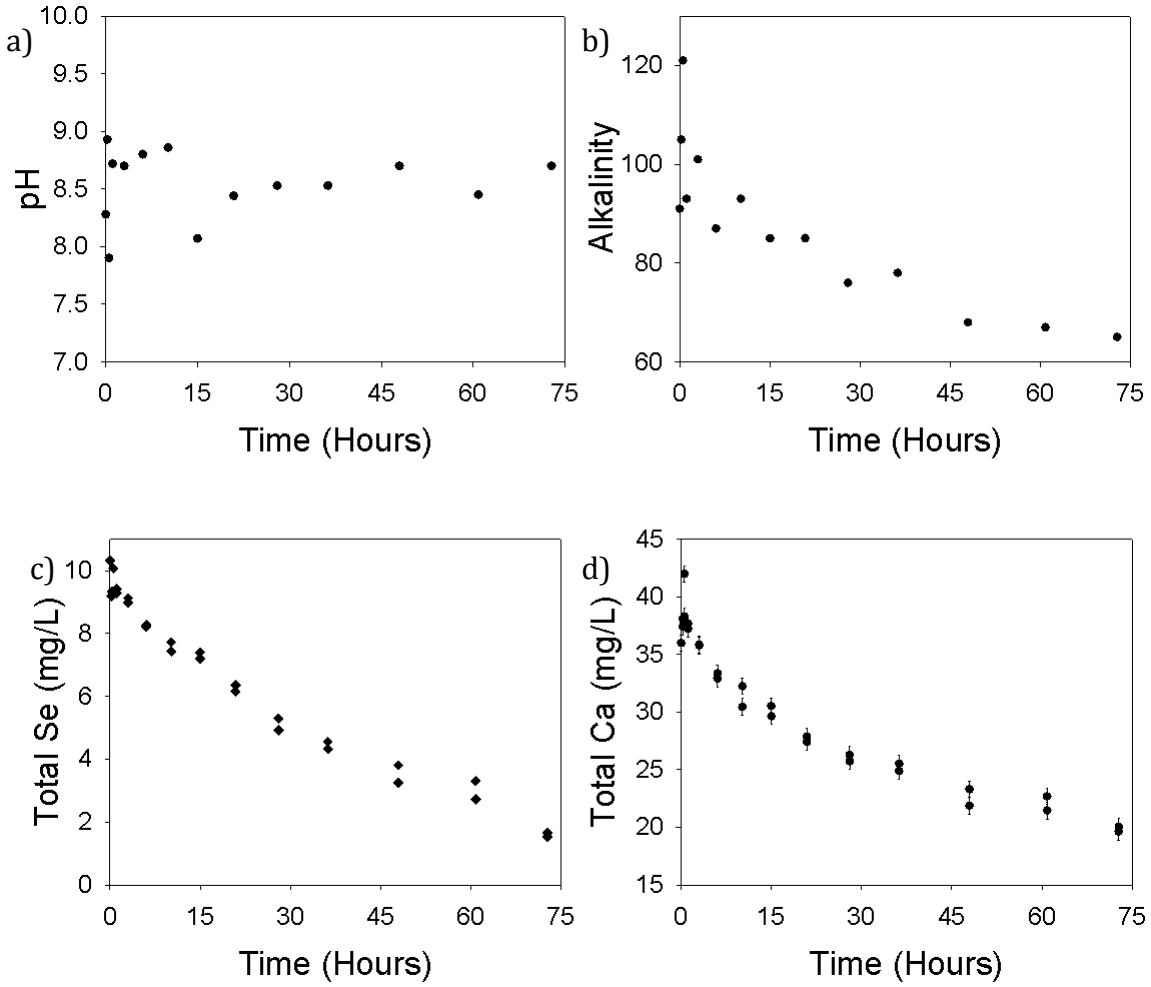

Figure 2.1: The variation in a few of the geochemical parameters over the length of the experiment: a) pH, b) alkalinity, and concentrations in solution of c) selenium and d) calcium. Error bars on selenium concentration measurements were smaller than the symbols, so were not included.

Selenium concentrations in solution decreased over time (Figure 2.1). There was little change in concentration relative to the Fe-free Se(VI) stock controls for the first 3 hrs. Replicate measurements differed by less than 0.9%. Duplicate samples differed in concentration by 18% at most for the two 60 hr samples, but on average by less than 6%. There was negligible Se(IV) in the stock solution, and there was no quantifiable Se(IV) in any of the filtered, un-acidified samples.

Measurements for Eh were fairly stable over time at about -450 mV, ranging between -471 mV to -258 mV with some scattered higher values. Reducing conditions prevailed throughout the experiments.

2.4.2 Solid sample analysis

The solid samples from the 15 minute, 10 hour, 21 hour, 36 hour, 48 hour, and 72 hour time steps were exposed to high energy X-rays at the APS for XANES analysis. Multiple scans were merged to reduce error, with 9 scans used for samples with lower concentrations of Se, and 6 scans used for the 21 hr sample onward. The spectra and standards are presented in figure 2.2. Most of the normalized scans are similar, though it is evident that the early times have a smaller shoulder before the main peak. All scans, except the 15 min scan, display two similarly sized peaks.

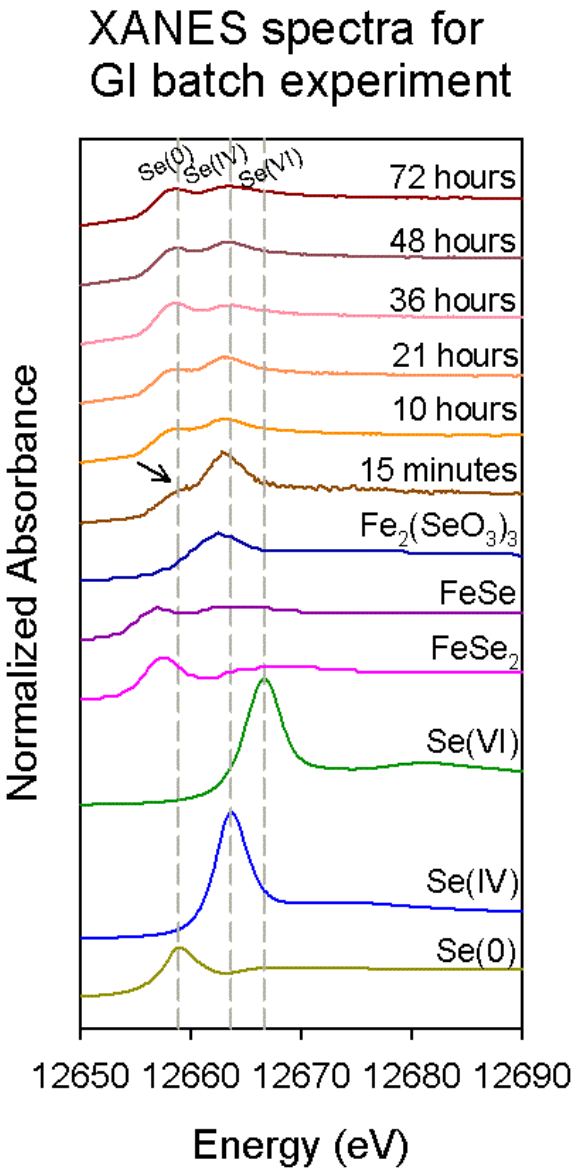

Figure 2.2: XANES scans from selected samples along the batch experiment time line. Standards used to determine the valence states composing each sample are on the bottom. Arrow points to lack of peak on 15 min sample.

The non-normalized scans (Figure 2.3) have increasing values for absorbance the longer the Fe was in contact with the Se-rich solution. The 21, 36, and 48 hour samples have approximately the same total absorbance, possibly due to the heterogeneity of Se on the GI.

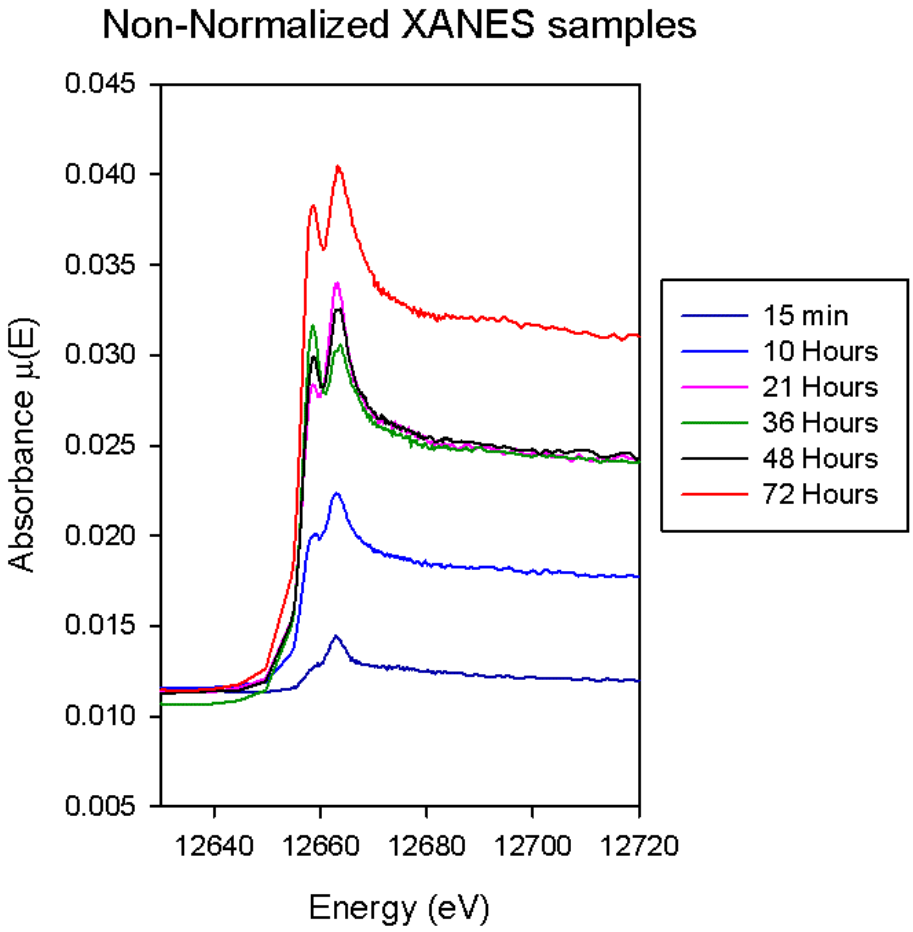

Figure 2.3: Non-normalized XANES scans from selected samples along the batch experiment time line. The difference in absorbance is related to the quantity of Se on the solid sample.

Linear combination fitting (LCF) was also conducted to determine the oxidation states of the Se on the iron (Table 2.1). The amount of Se(0) on the GI increased over time, while Se(IV) decreased. $Fe_2(SeO_3)_3$ began as the most major component, but also decreased over time. The selenide compounds $FeSe_2$ and FeSe are scarce in the earliest time step, but are present at similar percentages of the total Se on the GI for the remainder of the experiment. Se (VI) was not found on any of the samples. The difference between the data and the fit is presented in figures 2.4, 2.5, and 2.6.

Table 2.1: XANES fit from the program ATHENA for Se batch experiment using GI. No Se(VI) was found on any of the samples.

Time (hrs)	Se(0) (%)	Se(IV) (%)	$Fe_2(SeO_3)_3$ (%)	$FeSe_2$ (%)	FeSe (%)	Reduced χ^2
0.25	27.5	28.0	40.8	0.0	11.6	0.0808
10	28.3	11.8	20.8	15.7	24.8	0.0017
21	28.7	14.5	19.4	17.7	22.3	0.0022
36	42.7	12.7	1.1	29.6	14.8	0.0018
48	34.8	13.9	13.0	24.2	13.8	0.0016
72	31.7	9.7	8.4	21.3	29.9	0.0011

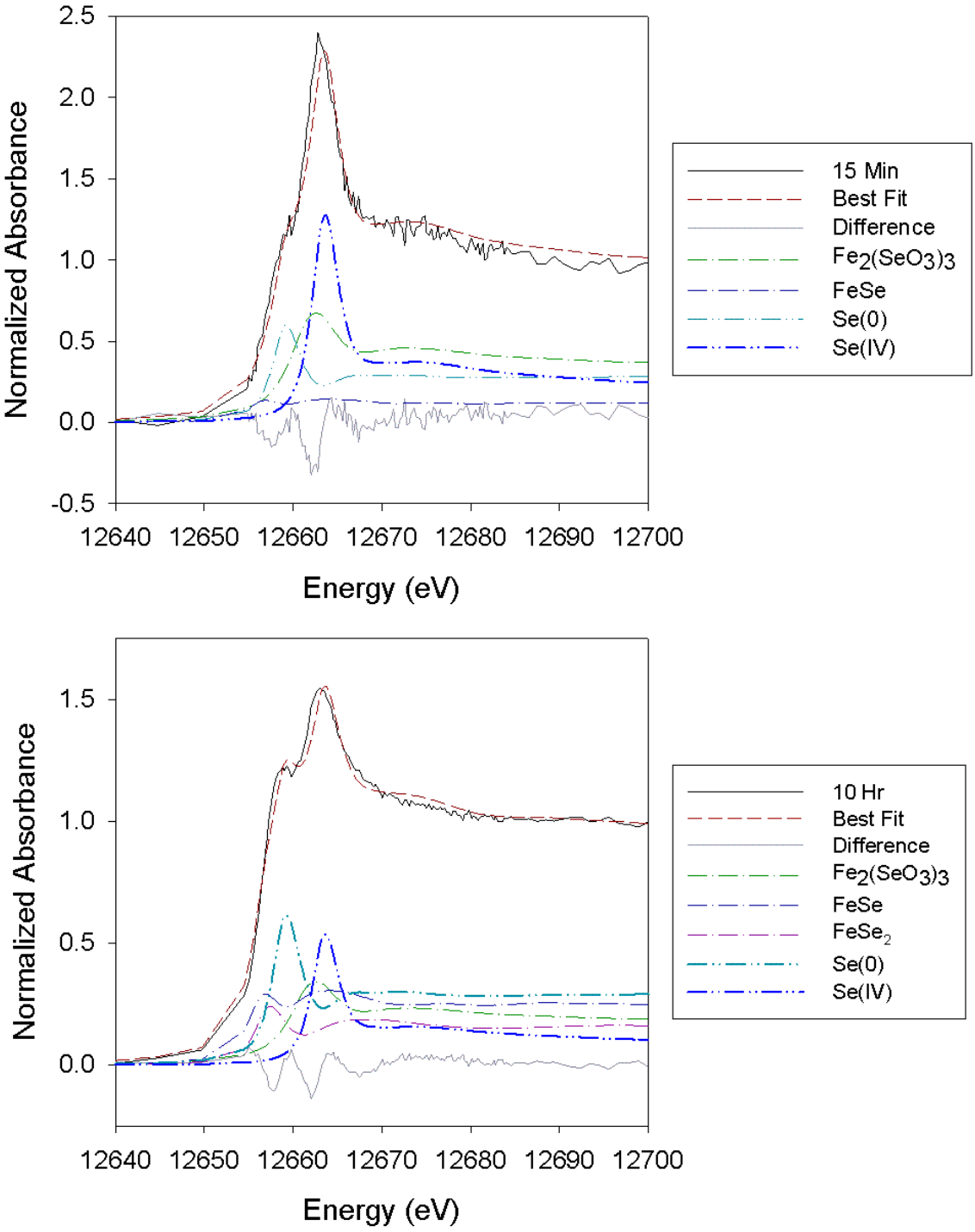

Figure 2.4: Linear combination fittings using Se(0), Se(IV), Se(VI), $FeSe_2$, FeSe, and $Fe_2(SeO_3)_3$, as well as the difference between the data and the best fit, for the 48 hr and 72 hr XANES samples.

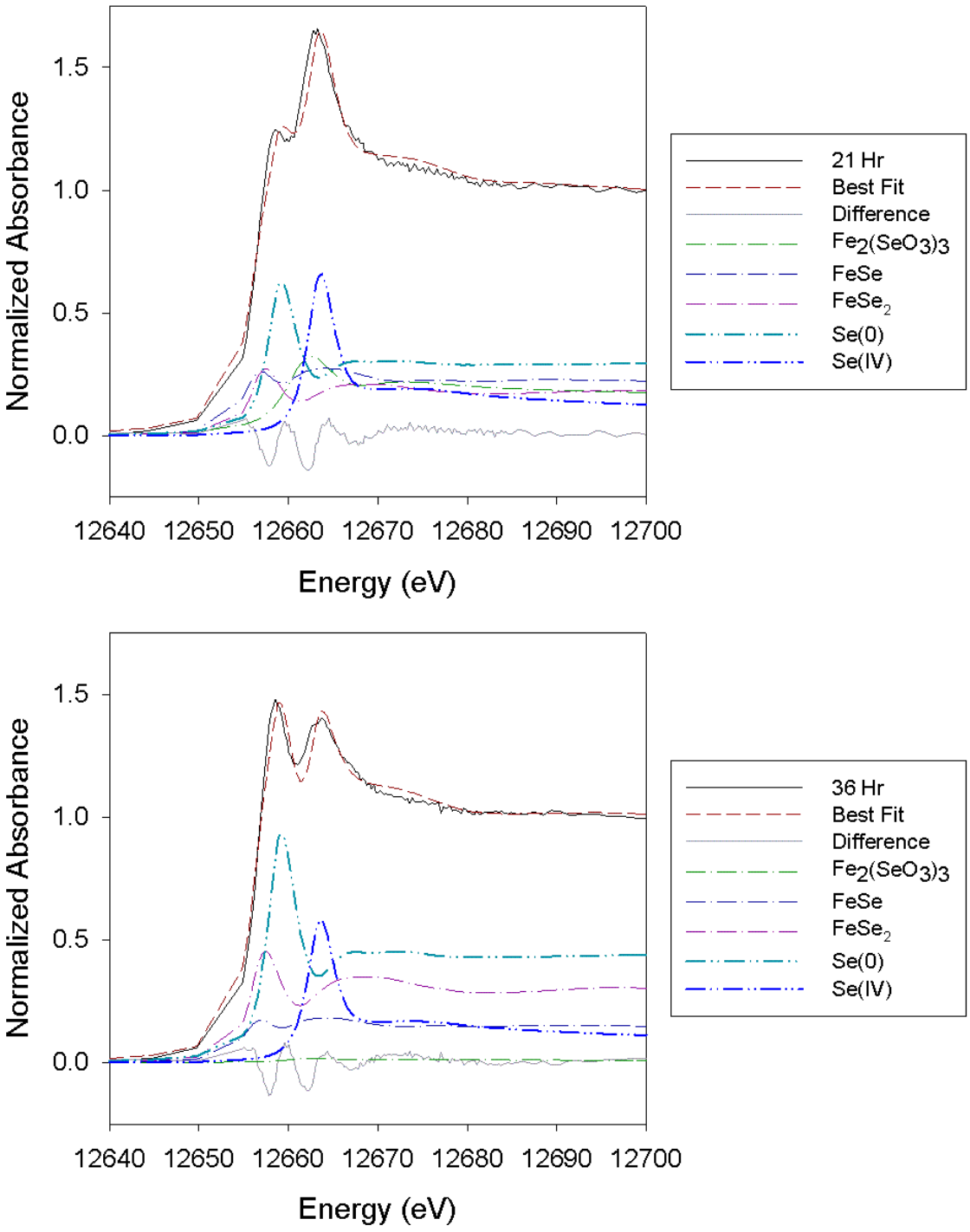

Figure 2.5: Linear combination fittings using Se(0), Se(IV), Se(VI), $FeSe_2$, FeSe, and $Fe_2(SeO_3)_3$, as well as the difference between the data and the best fit, for the 21 hr and 36 hr XANES samples.

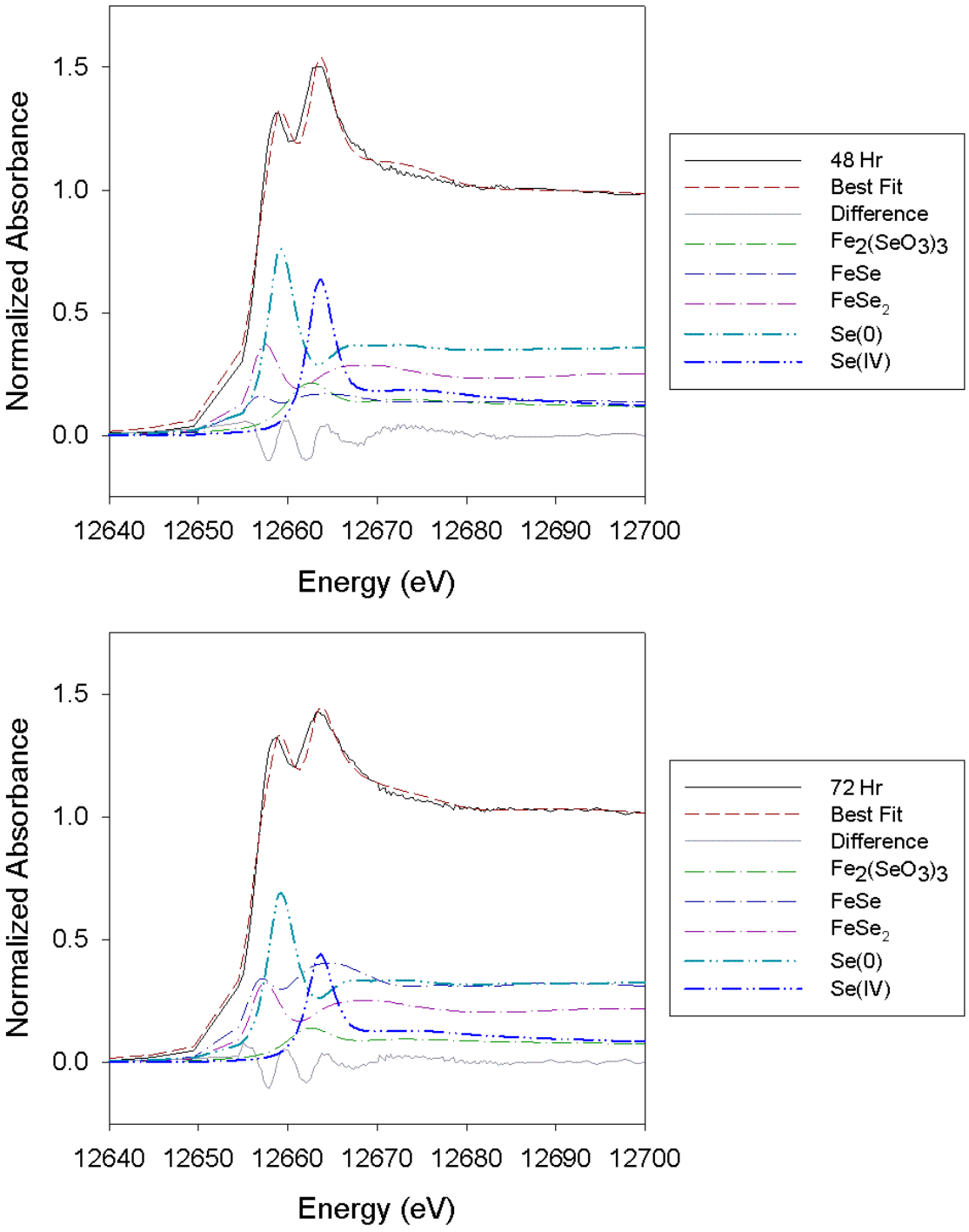

Figure 2.6: Linear combination fittings using Se(0), Se(IV), Se(VI), $FeSe_2$, FeSe, and $Fe_2(SeO_3)_3$, as well as the difference between the data and the best fit, for the 48 hr and 72 hr XANES samples.

2.4.3 Isotope results

Samples were analyzed to determine Se isotope ratios. Results were processed to obtain both $\delta^{82/78}$Se and $\delta^{82/76}$Se (Figure 2.7). The $\delta^{82/78}$Se and $\delta^{82/76}$Se values for the stock solution were -0.60 ± 0.09‰ and -0.94 ± 0.07‰ respectively. Delta values became more positive as the fraction of Se remaining in solution declined, with a maximum of 4.94 ± 0.17‰ $\delta^{82/78}$Se and 6.85 ± 0.52‰ $\delta^{82/76}$Se. Delta values began to decline after less than 14.5% of the original Se remained. A fractionation factor of 0.9970 was obtained using the Rayleigh model, with an R^2 value of 0.978 for $\delta^{82/78}$Se. For $\delta^{82/76}$Se, the fractionation factor is 0.9957, with an R^2 value of 0.983.

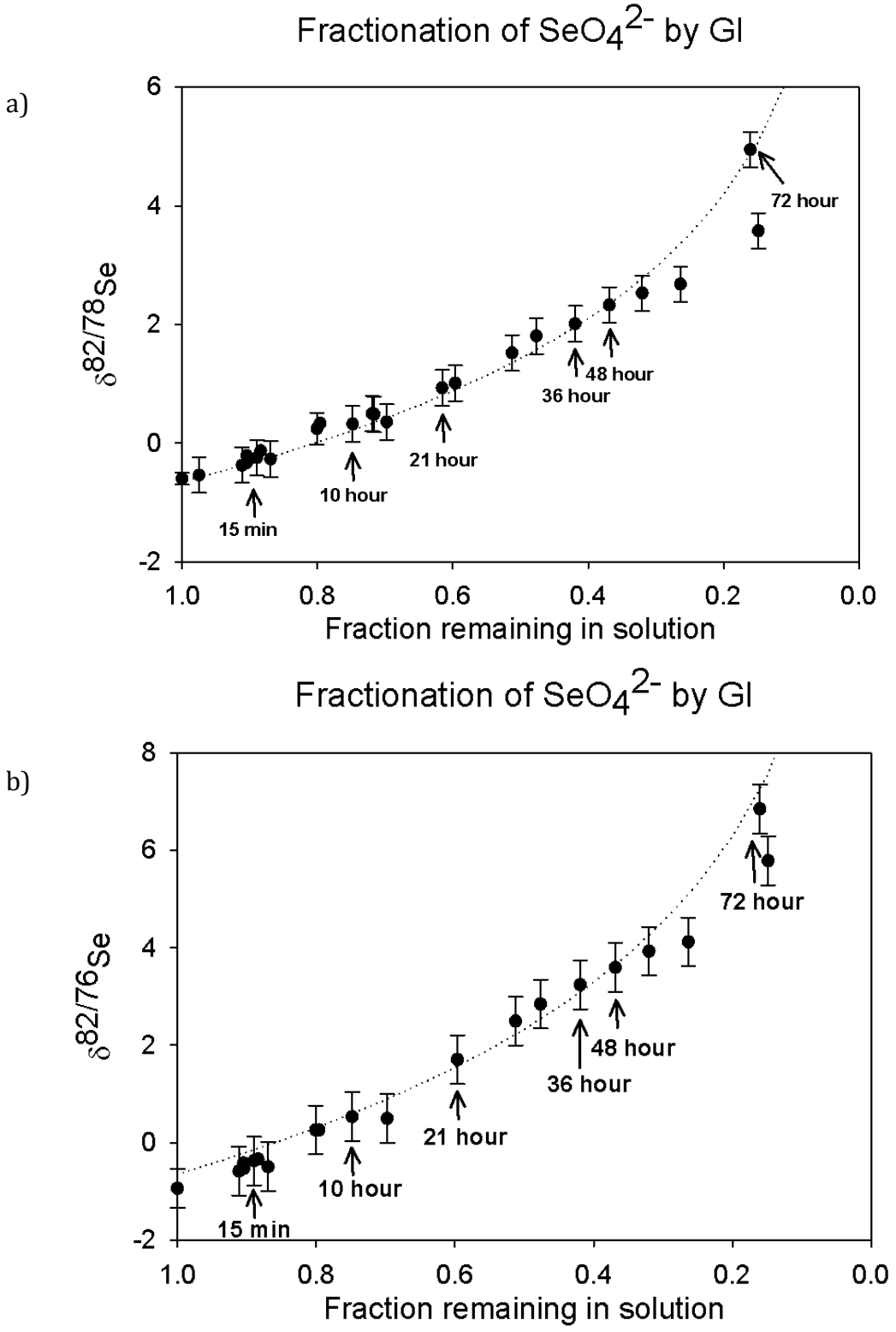

Figure 2.7: Se isotope results for the fractionation of Se(VI) by granular iron. a) The δ82/78Se values, and b) the δ82/76 values. Error bars represent the external reproducibility of the NIST SRM3149 (2σ), while the first error bar is the external reproducibility of the stock solution (2σ). Arrows in both diagrams point to the batch samples that were selected for XANES analysis.

2.5 Discussion

2.5.1 Geochemistry

2.5.1.1 Alkalinity, calcium, pH and Eh

The decrease in the concentration of Ca and the alkalinity of the solution over time is likely due to the precipitation of $CaCO_3$. Precipitation of $CaCO_3$ could cause a slight decrease in the porosity of the GI, potentially reducing permeability (Morrison et al. 2002). However, $CaCO_3$ precipitation is probably not detrimental to the reduction of Se by GI. Both Se(VI) and Se(IV) can co-precipitate with $CaCO_3$ (Aurelio et al. 2010; Chakraborty et al. 2010), potentially leading to the slight initial decrease in Se concentrations compared to the initial solution seen in both the early batch samples and the Fe-free controls. Because Ca is increasing in solution during this initial period, rather than decreasing, the removal mechanism is more likely sorption onto $CaCO_3$ and Fe rather than co-precipitation (Chakraborty et al. 2010; Goldberg and Glaubig 1988). Iron led to the reduction of Se(IV), even if Se is adsorbed onto Ca on the GI surface or directly on the surfaces of the GI (Chakraborty et al. 2010).

The concentration of dissolved Fe gradually increases, but remained below quantifiable concentrations. The detection of Fe at later times may be due to the lower availability of Se to react with, or simply the gradual oxidation of Fe. The concentration of Fe increasing in solution over time is not an unexpected outcome of mixing GI with water (Blowes et al. 2000; Morrison et al. 2002). Provided some Fe remains in solution, Se(IV) will remain on the solid phase, eventually reducing to more stable Se(0) (Charlet et al. 2007; Morrison et al. 2002).

The slight variability of pH measurements over time is likely due to the degassing of CO_2 in the stock solution. All the samples initiated at the beginning of the experiment had a lower pH, increased by the oxidation of Fe over time. Samples started later had lower concentrations of CO_2, and a slightly higher starting pH, which disrupted a clear trend. Degassing of CO_2 was indicated by the audible release of gas when an Fe-free selenium stock control was opened at the end of the experiment. The Ca concentration in this control sample was lower than the control measured at the start of the experiment, and the pH was 8.28. Regardless, the pH remained at about 8.6 after 28 hours. Other experiments using GI and $CaCO_3$ had a lower starting pH, but stabilized at a pH of 8.8 by 120 hours (Gibson et al. 2012).

The sorption of Se(VI) on Fe minerals is chemically similar to the behavior of sulfate (Davis and Leckie 1980). Although adsorption of Se(VI) on iron oxides is most extensive at pH < 7.5 (Davis and Leckie 1980), extensive sorption of Se(VI) is not anticipated in some systems with only negatively charged surfaces at any pH (Neal et al. 1987a).

Selenite sorption onto soil decreases at pH > 9 where Ca is present (Neal et al. 1987a). In the absence of Ca, the pH of maximum Se(IV) adsorption occurs within the pH range from 3 to 5 (Goldberg 2013). High pH conditions are not always ideal for the removal of Se by sorption alone, despite several studies centered around such methods (Mondal et al. 2004). Reduction is thus required for *in situ* removal of Se from a system.

The GI used for this experiment was pre-treated with $CaCO_3$ saturated water, and there was additional Ca in the stock solution. The presence of Ca affects the

extent of Se(IV) adsorption, increasing the extent of adsorption with increasing pH (Goldberg and Glaubig 1988; Neal et al. 1987b). In addition, the capacity of soils to retain Se(IV) is increased by the presence of Ca, even if more Se(IV) would be adsorbed at lower pH (Goldberg and Glaubig 1988).

Values for Eh indicate that reducing conditions were sustained in the batch reactor vessels throughout the experiment. The reduction of Se(IV) in solution can proceed even in the presence of some O_2 provided reducing conditions are maintained, demonstrating the potential for this system to remove Se in aerobic groundwater systems (Haudin et al. 2007; Liang et al. 2013). However, the presence of O_2 does impair the reduction of Se(VI) (Liang et al. 2013). Oxygen is only one of several factors, including high ionic strength and basic conditions, that decrease the rate of the Se(VI) reduction reaction (Amrhein et al. 1998). Note that the competition for electrons and the formation of iron oxides at the GI surface will limit the ability of Fe to reduce Se(VI) in the presence of O_2 (Qiu et al. 2000). Anoxic conditions provide more efficient treatment of Se, especially when it is present as Se(VI).

2.5.1.2 Selenium concentrations and speciation

Selenium was progressively removed from solution over time. Some Se(IV) may have been present in the original stock solution, explaining the rapid early decrease of about 500 μg/L in Se concentrations. After the initial decrease in concentration, Se(VI) concentrations did not change significantly over the next 6 hours, a slightly more rapid reaction rate for the reduction of Se(VI) by Fe than has been reported by others (Loyo et al. 2008). However, this study, unlike others,

included solutions saturated with $CaCO_3$, which may have increased the initial rate of the reaction by promoting electron transfer between Fe and Se (Chakraborty et al. 2010).

Negligible Se(IV) was present in solution throughout the experiment. Under the experimental conditions, it is likely that any Se(IV) generated by the reduction of Se(VI) rapidly adsorbed to the GI. Rapid adsorption of Se(IV) on Fe-containing minerals, including goethite, and hydrous ferric oxides has been observed, with reaction half-lives of less than 30 seconds, for pH from 3 to 8 (Zhang and Sparks 1990). While these minerals are not present in this system, they provide points for comparison.

2.5.1.3 Modeling of geochemical data

The geochemical data from the batch experiment was input into PHREEQCI to determine the speciation of Se and any likely precipitates once final equilibrium was reached. The dominant species present in solution were Se(-II), and Fe(II). The samples were supersaturated with respect to both calcite and siderite, as well as Se(0), $FeSe_2$, and several other Fe minerals (Table 2.2). $Fe_2(SeO_3)_3$ was not likely to be present by the end of the experiment, nor was $CaSeO_3$ or SeO_2.

Table 2.2: Saturation indexes of important phases. Results are from modeling experimental data using PHREEQCI.

Phase (Chemical Formula)	Saturation Index
Calcite ($CaCO_3$)	1.70
$CaSeO_3$	-18.11
Ferric selenite ($Fe_2(SeO_3)_3$)	-80.71
Ferroselite ($FeSe_2$)	9.41
Goethite (FeOOH)	5.32
Magnetite (Fe_3O_4)	19.65
$Se_{(s)}$	7.93
SeO_2	-33.2
Siderite	0.98

2.5.2 The solid phase

Selenium initially occurred predominantly as Se(IV) or $Fe_2(SeO_3)_3$ on the solid phase (Figures 2.2 & 2.3; Table 2). Elemental Se became more prevalent over time, and as the total quantity of Se on the Fe increased throughout the duration of the experiment (Figure 2.3). No Se(VI) was observed on the solid samples.

It is unlikely that iron selenite ($FeSeO_3$) formed, because the precipitation of this phase requires much higher concentrations of iron in solution, and is inhibited by the presence of Ca (Chakraborty et al. 2010). Ferric selenite ($Fe_2(SeO_3)_3$) was present, but it was replaced by more stable Fe-Se compounds over time. The abundance of ferroselite ($FeSe_2$) increased with time, and would be expected to remain stable under reducing conditions across a broad range of pH conditions (Morrison et al. 2002). XPS studies performed by others confirmed the presence of iron selenides, most likely as ferroselite ($FeSe_2$) during biotic reduction of Se(VI) in the presence of Fe (Sasaki et al. 2008a). Tetragonal iron selenide (FeSe) was also found on the iron, and may be less stable when the particle size is small (Scheinost and Charlet 2008). The lower stability of FeSe explains why it decreases in

prevalence on the GI over time after an initial increase. Experiments conducted using GI under aerobic conditions lack evidence of the presence of FeSe (Liang et al. 2013). It is possible that FeSe was recrystallizing into the more stable mineral achavalite (FeSe) over time, but the spectra are too similar for XANES analysis to be conclusive.

2.5.3 Isotopes

The combined solution and solid-phase analyses suggest that Se(VI) reduction is occurring in solution, followed by rapid adsorption to the GI surfaces, followed by more gradual reduction to Se(0) on the GI surface. This mechanism has been proposed by others (Chakraborty et al. 2010; Loyo et al. 2008). Little fractionation in Se isotopes is caused by Se(VI) or Se(IV) sorption (Mitchell et al. 2013; Schilling et al. 2013). Larger values for fractionation may be associated with the reduction of Se(VI) to Se(IV) (Johnson 2012).

The current measurements indicate a fractionation factor of $\varepsilon = \sim 3.0‰$ for $^{82/78}Se$ and $\varepsilon = \sim 4.3‰$ for $^{82/76}Se$. This fractionation factor is much larger than the fractionation factor of reported 0.8‰ for sorption (Johnson et al. 1999; Johnson and Bullen 2004), or the value of less than 1.0‰ found by Mitchell et al. (2013a) in an experiment containing only Se(IV). The fractionation factor measured in the current experiments is much closer to the value obtained for the reduction of Se(VI) to Se(IV) in a sediment slurry of 3.9–4.7‰ (Ellis et al. 2003), and is also close to the values reported for microbially mediated reduction of Se(VI) to Se(IV) (Herbel et al. 2000). The similarity in fractionation factors observed for abiotic and biologically mediated reduction of Se(VI) to Se(IV) suggests that it may be difficult to discern the

exact reduction mechanism in natural systems through Se isotope measurements (Clark and Johnson 2010).

The effective fractionation established in this study is not as large as has been found in other abiotic reduction experiments, such as those using green rust (Johnson and Bullen 2003), pyrite (Mitchell et al. 2013), or concentrated hydrochloric acid (Johnson et al. 1999; Rees and Thode 1966). These reactions may also include some reduction to Se(0), which would increase the degree of fractionation. Reduction from Se(VI) to Se(IV) typically produces less fractionation than reduction from Se(IV) to Se(0) (Herbel et al. 2000; Johnson 2012).

Combined, our observations of aqueous concentrations and speciation, solid-phase speciation and isotope ratio measurements suggest that Se(VI) reduction to Se(IV) occurred in solution, followed by adsorption to the GI surface. Selenite on the GI surface was then reduced, progressively producing more Se(0), as indicated by the XANES spectra (Figure 2.3). The second reduction step occurred in isolation from the aqueous phase, thus resulting in a lower overall degree of fractionation than previously observed for direct reduction of Se(VI) to Se(0).

2.6 Summary

The low Se(IV) concentrations in solution, and lack of Se(VI) on the solid phase combined with the increase of Se(IV), Se(0), and iron selenides suggests that Se(VI) reduction to Se(IV) occurred in solution, followed by sorption to the solid phase (Loyo et al. 2008; Mitchell et al. 2013; Schilling et al. 2013). This reduction created a measurable fractionation, starting with values of -0.60 ± 0.09‰ and -0.94 ± 0.07‰ in the stock solution, and reaching 4.94 ± 0.17‰ and 6.85 ± 0.52‰ after

72 hours for $\delta^{82/78}$Se and $\delta^{82/76}$Se, respectively. The presence of Ca on the GI surface likely enhanced the sorption of Se(IV), leading to less abiotic reduction in solution, and lower effective fractionation than reported by others.

The direct reduction of Se(VI) by GI is possible, if sluggish. Recent studies suggest that using nano-particles of Fe increases the rate of reaction (Loyo et al. 2008). Adding Ca to the nano-particles would likely accelerate this reaction, due to increased adsorption of Se(IV) (Chakraborty et al. 2010). No stable Se isotope studies have as of yet been performed when the reducing material is nano-particulate Fe.

The results from this study only cover the reduction of Se(VI) under static (batch) conditions. The degree of fractionation may differ under dynamic flow conditions. Column studies would help to verify the usefulness of Se isotopes as an indicator of Se removal mechanisms under normal groundwater flow conditions.

Chapter 3:

Conclusions

Established methods were modified to measure Se isotope ratios by HG-MC-ICP-MS. Fractionation caused by the reduction of Se(VI) by GI is measurably greater than the error associated with Se isotope measurements. Purification using TCF successfully removed the interferences of greatest concern. The data reduction method used included mathematical corrections to remove interferences from other elements, dimers, and hydrides.

Granular iron is commonly used in PRB systems to remove dissolved contaminants, including Se. Although previous studies have examined the extent of Se isotope fractionation associated with natural materials, including green rust, pyrite, mackinawite and iron oxides, few isotope studies have focused on reduction by GI. The results from the current experiments indicate low Se(IV) concentrations in solution, and no Se(VI) on the solid phase. These observations, combined with increases of both Se(IV), Se(0), and iron selenides on the solid phase, suggest that Se(VI) reduction to Se(IV) is occurring in solution, followed by sorption to the GI surface. Measurable fractionations, starting with values of -0.60 ± 0.09‰ and -0.94 ± 0.07‰ in the stock solution, and reaching 4.94 ± 0.17‰ and 6.85 ± 0.52‰ after 72 hours for $\delta^{82/78}$Se and $\delta^{82/76}$Se, respectively, suggest that the presence of Ca at the GI surface likely enhanced the sorption of Se(IV), leading to less reduction in solution, and lower effective fractionation than reported by others. These observations indicate that measurements of Se isotope ratios have potential to

augment measurements of Se concentrations to elucidate Se removal mechanism in groundwater remediation systems.

Chapter 4:

Recommendations for Future Research

Multiple studies have been conducted on the removal of Se by a variety of mechanisms and materials (Lenz and Lens 2009; Mondal et al. 2004). There has been a particularly large focus placed on adsorption studies on local soils, as there is concern for both migration of high concentrations of Se, and availability of low concentrations (Dhillon and Dhillon 1999; Schilling et al. 2011b). Far less work has been done on *in situ* remediation, and many experiments do not include Se(VI). A large portion of the studies conducted on zero-valent iron either do not use GI (Morrison et al. 2002; Qiu et al. 2000), have a very different grain size or composition (Loyo et al. 2008; Mondal et al. 2004), or are aerobic (Liang et al. 2013).

Current research on Se isotope fractionation remains sparse. Research on fractionation in the environment is equally rare. Although GI may not exist naturally in a system, chapter two presents information that may be useful in assessing the removal of Se by an Fe PRB. Some isotope work has been done on the reduction of Se by Fe minerals that may be found in the ground such as green rust, pyrite, mackinawite, and several iron oxides (Johnson et al. 1999; Mitchell et al. 2013). These materials may not be found in all systems, or with the same water chemistry used in the experiments, so the precise extent of fractionation that will occur will probably be site dependent. Work done on biotic reduction in the laboratory and in the field has already confirmed this hypothesis (Clark and Johnson 2008; Clark and Johnson 2010; Ellis et al. 2003). Length of flow path for groundwater, local

processes, and the different biota present all contribute to reduction and thus different degrees of fractionation (Schilling et al. 2013; Wen and Carignan 2011). Additional research, including field research, should be conducted. Furthermore, column experiments should be done to elucidate whether flow has a direct effect on Se isotope fractionation.

Selenium oxyanions are commonly found alongside S in the environment (Lenz and Lens 2009). The addition of SO_4^{2-} to the system appears to have an ambiguous affect, potentially increasing the reaction rate in some cases (Gibson et al. 2012), and decreasing it in others (Mondal et al. 2004), possibly due to competition for sorption sites (Winkel et al. 2012). One study found that S itself had no effect, but other elements added in order to obtain the S diminished the treatment of Se (Neal et al. 1987b). Column and batch experiments have been done using GI with solutions also containing S (Gibson et al. 2012; Sasaki et al. 2008), but isotope analysis for Se was not performed on the samples. The presence of S did seem to lead to an increased reduction rate in those studies. A system containing both Fe and S, in the form of pyrite (FeS_2) has been studied in batch form for Se isotopes, and removal of Se(IV) took about a day (Mitchell et al. 2013a). Removal of Se(IV) from solution in this study using both Ca and Fe was almost instantaneous, so the effect of S remains somewhat ambiguous.

Other common compounds have been found to have a larger effect on Se(VI) removal than S. Phosphates tend to desorb Se(VI) from soils (Goh and Lim 2004; Neal et al. 1987b), and nitrates have been found to oxidize already reduced forms of Se, or prevent reduction (Gates et al. 2003). Neither sorption nor oxidation are

theorized to result in large quantities of fractionation (Johnson and Bullen 2004), but the studies have yet to be performed.

References

Amouroux D, Donard OFX (1997) Evasion of selenium to the atmosphere via biomethylation processes in the Gironde estuary, France. Mar Chem 58:173–188. doi: 10.1016/S0304-4203(97)00033-9

Amrhein C, Hunt M, Roberson M, et al. (1998) The use of XANES, STM, and XPS to identify the precipitation products formed during the reaction of U, Cr, and Se with zero-valent iron. Goldschmidt Conf. T oulouse. Toulouse, pp 51–52

Aurelio G, Fernández-Martínez a., Cuello GJ, et al. (2010) Structural study of selenium(IV) substitutions in calcite. Chem Geol 270:249–256. doi: 10.1016/j.chemgeo.2009.12.004

Basu R, Haque S, Tang J, et al. (2007) Evolution of selenium concentrations and speciation in groundwater flow systems: Upper Floridan (Florida) and Carrizo Sand (Texas) aquifers. Chem Geol 246:147–169. doi: 10.1016/j.chemgeo.2007.09.010

Blowes DW, Ptacek CJ, Benner SG, et al. (2000) Treatment of inorganic contaminants using permeable reactive barriers. J Contam Hydrol 45:123–137. doi: 10.1016/S0169-7722(00)00122-4

Boult K, Cowper M, Heath T, et al. (1998) Towards an understanding of the sorption of U (VI) and Se (IV) on sodium bentonite. J Contam Hydrol 35:141–150.

Breynaert E, Scheinost AC, Dom D, et al. (2010) Reduction of Se(IV) in boom clay: XAS solid phase speciation. Environ Sci Technol 44:6649–55. doi: 10.1021/es100569e

Brimmer SP, Fawcett WR, Kulhavy KA (1987) Quantitative Reduction of Selenate Ion to Selenite in Aqueous Samples. Anal Chem 59:1470–1471.

Bye R, Lund W (1988) Optimal conditions for the reduction of selenate to selenite by hydrochloric acid. Anal Chemie 332:242–244. doi: 10.1007/BF00492968

Carignan J, Wen H (2007) Scaling NIST SRM 3149 for Se isotope analysis and isotopic variations of natural samples. Chem Geol 242:347–350. doi: 10.1016/j.chemgeo.2007.03.020

Chakraborty S, Bardelli F, Charlet L (2010) Reactivities of Fe(II) on calcite: selenium reduction. Environ Sci Technol 44:1288–94. doi: 10.1021/es903037s

Charlet L, Scheinost a. C, Tournassat C, et al. (2007) Electron transfer at the mineral/water interface: Selenium reduction by ferrous iron sorbed on clay. Geochim Cosmochim Acta 71:5731–5749. doi: 10.1016/j.gca.2007.08.024

Clark SK, Johnson T (2008) Effective isotopic fractionation factors for solute removal by reactive sediments: A laboratory microcosm and slurry study. Environ Sci Technol 42:7850–7855.

Clark SK, Johnson TM (2010) Selenium stable isotope investigation into selenium biogeochemical cycling in a lacustrine environment: Sweitzer Lake, Colorado. J Environ Qual 39:2200–2210. doi: 10.2134/jeq2009.0380

Conde JE, Sanz Alaejos M (1997) Selenium concentrations in natural and environmental waters. Chem Rev 97:1979–2004.

Davis JA, Leckie JO (1980) Surface Ionization and Complexation at the Oxide/Water Interface: 3. Adsorption of Anions. J Colloid Interface Sci 74:32–43.

Dhillon K., Dhillon S. (1999) Adsorption–desorption reactions of selenium in some soils of India. Geoderma 93:19–31. doi: 10.1016/S0016-7061(99)00040-3

Van Dyke JU, Hopkins W a, Jackson BP (2013) Influence of relative trophic position and carbon source on selenium bioaccumulation in turtles from a coal fly-ash spill site. Environ Pollut 182C:45–52. doi: 10.1016/j.envpol.2013.06.025

Ellis AS, Johnson TM, Herbel MJ, Bullen TD (2003) Stable isotope fractionation of selenium by natural microbial consortia. Chem Geol 195:119–129. doi: 10.1016/S0009-2541(02)00391-1

Elrashidi MA, Adriano DC, Workman SM, Lindsay WL (1987) Chemical equilibria of selenium in soils; a theoretical development. Soil Sci 144:141–152.

Elwaer N, Hintelmann H (2007) Comparative performance study of different sample introduction techniques for rapid and precise selenium isotope ratio determination using multi-collector inductively coupled plasma mass spectrometry (MC-ICP/MS). Anal Bioanal Chem 389:1889–99. doi: 10.1007/s00216-007-1537-z

Elwaer N, Hintelmann H (2008a) Selective separation of selenium (IV) by thiol cellulose powder and subsequent selenium isotope ratio determination using multicollector inductively coupled plasma. J Anal At Spectrom 23:733–743. doi: 10.1039/b801673a

Elwaer N, Hintelmann H (2008b) Precise selenium isotope ratios measurement using a multimode sample introduction system (MSIS) coupled with multicollector inductively coupled plasma mass spectrometry (MC-ICP-MS). J Anal At Spectrom 23:1392–1396. doi: 10.1039/b808645c

Fernández-Martínez A, Charlet L (2009) Selenium environmental cycling and bioavailability: a structural chemist point of view. Rev Environ Sci Biotechnol 8:81–110. doi: 10.1007/s11157-009-9145-3

Gates TK, Cody BM, Donnelly JP, et al. (2003) Assessing selenium contamination in the irrigated stream-aquifer system of the Arkansas River, Colorado. J Environ Qual 38:2344–56. doi: 10.2134/jeq2008.0499

Gibson BD, Blowes DW, Lindsay MBJ, Ptacek CJ (2012) Mechanistic investigations of Se(VI) treatment in anoxic groundwater using granular iron and organic carbon: an EXAFS study. J Hazard Mater 241-242:92–100. doi: 10.1016/j.jhazmat.2012.09.015

Goh K-H, Lim T-T (2004) Geochemistry of inorganic arsenic and selenium in a tropical soil: effect of reaction time, pH, and competitive anions on arsenic and selenium adsorption. Chemosphere 55:849–59. doi: 10.1016/j.chemosphere.2003.11.041

Goldberg S (2013) Modeling selenite adsorption envelopes on oxides, clay minerals, and soils using the triple layer model. Soil Sci Soc Am J 77:64–71. doi: 10.2136/sssaj2012.0205

Goldberg S, Glaubig R (1988) Anion sorption on a calcareous, montmorillonitic soil – Selenium. Soil Sci Soc Am J 52:954–958.

Goossens J, Moens L, Dams R (1994) A mathematical correction method for spectral interferences on selenium in inductively coupled plasma mass spectrometry. Talanta 41:187–93.

Haudin CS, Renault P, Leclerc-Cessac E, Staunton S (2007) Effect of selenite additions on microbial activity and dynamics in three soils incubated under aerobic conditions. Soil Biol Biochem 39:2670–2674. doi: 10.1016/j.soilbio.2007.04.020

Hayes KF, Roe AL, Brown GEJ, et al. (1987) In situ X-ray absorption study of surface complexes: selenium oxyanions on alpha-FeOOH. Science (80-) 238:783–786.

Herbel MJ, Johnson TM, Oremland RS, Bullen TD (2000) Fractionation of selenium isotopes during bacterial respiratory reduction of selenium oxyanions. Geochim Cosmochim Acta 64:3701–3709.

Herbel MJ, Johnson TM, Tanji KK, et al. (2002) Selenium stable isotope ratios in california agricultural drainage water management systems. J Environ Qual 31:1146–1156. doi: 10.2134/jeq2002.1146

Hopkins WA, DuRant SE, Staub BP, et al. (2005) Reproduction, Embryonic Development, and Maternal Transfer of Contaminants in the Amphibian Gastrophryne carolinensis. Environ Health Perspect 114:661–666. doi: 10.1289/ehp.8457

Jamieson-Hanes JH, Gibson BD, Lindsay MBJ, et al. (2012) Chromium isotope fractionation during reduction of Cr(VI) under saturated flow conditions. Environ Sci Technol 46:6783–9. doi: 10.1021/es2042383

Johnson T (2004) A review of mass-dependent fractionation of selenium isotopes and implications for other heavy stable isotopes. Chem Geol 204:201–214. doi: 10.1016/j.chemgeo.2003.11.015

Johnson TM (2012) Stable isotopes of Cr and Se as tracers of redox processes in earth surface environments. In: Baskaran M (ed) Handb. Environ. Isot. Geochemistry. Springer Berlin Heidelberg, Berlin, Heidelberg, pp 155–175

Johnson TM, Bullen TD (2004) Mass-dependent fractionation of selenium and chromium isotopes in low-temperature environments. Rev Mineral Geochemistry 55:289–317.

Johnson TM, Bullen TD (2003) Selenium isotope fractionation during reduction by Fe (II)-Fe (III) hydroxide-sulfate (green rust). Science (80-) 67:413– 419.

Johnson TM, Herbel MJ, Bullen TD, Zawislanski PT (1999) Selenium isotope ratios as indicators of selenium sources and oxyanion reduction. Geochim Cosmochim Acta 63:2775–2783.

Kent D, Davis J, Anderson L, Rea B (1994) Transport of chromium and selenium in the suboxic zone of a shallow aquifer: Influence of redox and adsorption reactions. Water Resour Res 30:1099–1114.

Kim SS, Min JH, Lee JK, et al. (2012) Effects of pH and anions on the sorption of selenium ions onto magnetite. J Environ Radioact 104:1–6. doi: 10.1016/j.jenvrad.2011.09.013

Krouse H, Thode H (1962) Thermodynamic properties and geochemistry of isotopic compounds of selenium. Can J Chem 40:367–375.

De Laeter J, Böhlke J, De Bièvre P, et al. (2003) Atomic weights of the elements: Review 2000 (IUPAC Technical Report). Pure Appl Chem 75:683–800.

Layton-Matthews D, Leybourne MI, Peter JM, Scott SD (2006) Determination of selenium isotopic ratios by continuous-hydride-generation dynamic-reaction-cell inductively coupled plasma-mass spectrometry. J Anal At Spectrom 21:41–49. doi: 10.1039/b501704a

Lemly a D (2004) Aquatic selenium pollution is a global environmental safety issue. Ecotoxicol Environ Saf 59:44–56. doi: 10.1016/S0147-6513(03)00095-2

Lemly a D (2002) Symptoms and implications of selenium toxicity in fish: the Belews Lake case example. Aquat Toxicol 57:39–49.

Lenz M, Lens PNL (2009) The essential toxin: the changing perception of selenium in environmental sciences. Sci Total Environ 407:3620–33. doi: 10.1016/j.scitotenv.2008.07.056

Levander OA, Burk RF (2006) Update of human dietary standards for selenium. In: Hatfield DL, Berry MJ, Gladyshev VN (eds) Selenium Its Mol. Biol. Role Hum. Heal., Second Edi. Springer, New York, pp 399–410

Liang L, Yang W, Guan X, et al. (2013) Kinetics and mechanisms of pH-dependent selenite removal by zero valent iron. Water Res. doi: 10.1016/j.watres.2013.07.011

Loyo RLDA, Nikitenko SI, Scheinost AC, Simonoff M (2008) Immobilization of selenite on Fe3O4 and Fe/Fe3C ultrasmall particles. Environ Sci Technol 42:2451–6.

Martens D, Suarez D (1997) Selenium speciation of soil/sediment determined with sequential extractions and hydride generation atomic absorption spectrophotometry. Environ Sci Technol 31:133–139.

Missana T, Alonso U, Scheinost a. C, et al. (2009) Selenite retention by nanocrystalline magnetite: Role of adsorption, reduction and dissolution/co-precipitation processes. Geochim Cosmochim Acta 73:6205–6217. doi: 10.1016/j.gca.2009.07.005

Mitchell K, Couture R-M, Johnson TM, et al. (2013) Selenium sorption and isotope fractionation: Iron(III) oxides versus iron(II) sulfides. Chem Geol 342:21–28. doi: 10.1016/j.chemgeo.2013.01.017

Mitchell K, Mason PRD, Van Cappellen P, et al. (2012) Selenium as paleo-oceanographic proxy: A first assessment. Geochim Cosmochim Acta 89:302–317. doi: 10.1016/j.gca.2012.03.038

Mondal K, Jegadeesan G, Lalvani SB (2004) Removal of selenate by Fe and NiFe nanosized particles. Ind Eng Chem Res 43:4922–4934. doi: 10.1021/ie0307151

Morrison SJ, Goodknight CS, Tigar AD, et al. (2012) Naturally occurring contamination in the Mancos Shale. Environ Sci Technol 46:1379–87. doi: 10.1021/es203211z

Morrison SJ, Metzler DR, Dwyer BP (2002) Removal of As, Mn, Mo, Se, U, V and Zn from groundwater by zero-valent iron in a passive treatment cell: reaction progress modeling. J Contam Hydrol 56:99–116.

Neal RH, Sposito G, Holtzclaw K, Traina S (1987a) Selenite adsorption on alluvial soils: I. Soil composition and pH effects. Soil Sci Soc Am J 51:1161–1165.

Neal RH, Sposito G, Holtzclaw K, Traina S (1987b) Selenite adsorption on alluvial soils: II. Solution composition effects. Soil Sci Soc Am J 51:1165–1169.

Peak D, Sparks DL (2002) Mechanisms of selenate adsorption on iron oxides and hydroxides. Environ Sci Technol 36:1460–6.

Peters G, Maher W, Jolley D, et al. (1999) Selenium contamination, redistribution and remobilisation in sediments of Lake Macquarie, NSW. Org Geochem 30:1287–1300.

Plant J, Kinniburgh D, Smedley P, et al. (2003) Arsenic and selenium. Treatise on Geochemistry, Plan. Elsevier Ltd, Keyworth, Nottingham, UK, pp 17–66

Qiu SR, Lai H-F, Roberson MJ, et al. (2000) Removal of Contaminants from Aqueous Solution by Reaction with Iron Surfaces. Langmuir 16:2230–2236. doi: 10.1021/la990902h

Rashid K, Krouse HR (1985) Selenium isotopic fractionation during SeO3-2 reduction to Se(0) and H2Se. Can J Chem 63:3195–3199.

Ravel B, Newville M (2005) ATHENA, ARTEMIS, HEPHAESTUS: data analysis for X-ray absorption spectroscopy using IFEFFIT. J Synchrotron Radiat 12:537–41. doi: 10.1107/S0909049505012719

Rees CE, Thode HG (1966) Selenium isotope effects in the reduction of sodium selenite and of sodium selenate. Can J Chem 44:419–427.

Rouxel O, Ludden J, Carignan J, et al. (2000) Natural variations of selenium isotopes determined by multicollector plasma source mass spectrometry. Geoanalysis 2000. pp 43–44

Rouxel O, Ludden J, Carignan J, et al. (2002) Natural variations of Se isotopic composition determined by hydride generation multiple collector inductively coupled plasma mass spectrometry. Geochim Cosmochim Acta 66:3191–3199.

Rovira M, Giménez J, Martínez M, et al. (2008) Sorption of selenium(IV) and selenium(VI) onto natural iron oxides: goethite and hematite. J Hazard Mater 150:279–84. doi: 10.1016/j.jhazmat.2007.04.098

Rudge JF, Reynolds BC, Bourdon B (2009) The double spike toolbox. Chem Geol 265:420–431. doi: 10.1016/j.chemgeo.2009.05.010

Sasaki K, Blowes DW, Ptacek CJ (2008a) Spectroscopic study of precipitates formed during removal of selenium from mine drainage spiked with selenate using permeable reactive materials. Geochem J 42:283–294.

Sasaki K, Blowes DW, Ptacek CJ, Gould WD (2008b) Immobilization of Se(VI) in mine drainage by permeable reactive barriers: column performance. Appl Geochemistry 23:1012–1022. doi: 10.1016/j.apgeochem.2007.08.007

Scheinost AC, Charlet L (2008) Selenite reduction by mackinawite, magnetite and siderite: XAS characterization of nanosized redox products. Environ Sci Technol 42:1984–9.

Scheinost AC, Kirsch R, Banerjee D, et al. (2008) X-ray absorption and photoelectron spectroscopy investigation of selenite reduction by FeII-bearing minerals. J Contam Hydrol 102:228–45. doi: 10.1016/j.jconhyd.2008.09.018

Scheinost AC, Schmeisser N, Banerjee D, et al. (2013) AcXAS An Actinide Refernece X-ray Absorption Spectroscopy Database. https://www.hzdr.de/acxa.

Schilling K, Johnson TM, Wilcke W (2011a) Isotope fractionation of selenium during fungal biomethylation by Alternaria alternata. Environ Sci Technol 45:2670–6. doi: 10.1021/es102926p

Schilling K, Johnson TM, Wilcke W (2011b) Selenium partitioning and stable isotope ratios in urban topsoils. Soil Sci Soc Am J 75:1354. doi: 10.2136/sssaj2010.0377

Schilling K, Johnson TM, Wilcke W (2013) Isotope fractionation of selenium by biomethylation in microcosm incubations of soil. Chem Geol 352:101–107. doi: 10.1016/j.chemgeo.2013.05.013

Schilling K, Wilcke W (2010) A method to quantitatively trap volatilized organoselenides for stable selenium isotope analysis. J Environ Qual 40:1021–7. doi: 10.2134/jeq2010.0474

Séby F, Potin-Gautier M, Giffaut E, et al. (2001) A critical review of thermodynamic data for selenium species at 25˚C. Chem Geol 171:173–194.

Siebert C, Nägler TF, Kramers JD (2001) Determination of molybdenum isotope fractionation by double-spike multicollector inductively coupled plasma mass spectrometry. Geochemistry Geophys. Geosystems 2:

Torres J, Pintos V, Domínguez S, et al. (2010) Selenite and selenate speciation in natural waters: Interaction with divalent metal ions. J Solution Chem 39:1–10. doi: 10.1007/s10953-009-9491-3

USA EPA (1996) Proposed Selenium Criterion Maximum Concentration for the Water Quality Guidance for the Great Lakes System. 61:58444–58449.

Wen H, Carignan J (2011) Selenium isotopes trace the source and redox processes in the black shale-hosted Se-rich deposits in China. Geochim Cosmochim Acta 75:1411–1427. doi: 10.1016/j.gca.2010.12.021

White AF, Benson SM, Yee AW, et al. (1991) Groundwater contamination at the Kesterson Reservoir, California 2. Geochemical Parameters Influencing Selenium Mobility. Water Resour Res 27:1085–1098.

Winkel LHE, Johnson CA, Lenz M, et al. (2012) Environmental selenium research: from microscopic processes to global understanding. Environ Sci Technol 46:571–9. doi: 10.1021/es203434d

Young TF, Finley K, Adams WJ, et al. (2010) What you need to know about selenium. In: Chapman P (ed) Ecol. Assess. Selenium Aquat. Environ. SETAC Press, Pensacola, pp 7–45

Yu M, Tian W, Sun D, et al. (2001) Systematic studies on adsorption of 11 trace heavy metals on thiol cotton fiber. Anal Chim Acta 428:209–218. doi: 10.1016/S0003-2670(00)01238-1

Zhang P, Sparks D (1990) Kinetics of selenate and selenite adsorption/desorption at the goethite/water interface. Environ Sci Technol 24:1848–1856.

Zhu J, Johnson T, Clark S, Zhu X (2008) High precision measurement of selenium isotopic composition by hydride generation multiple collector inductively coupled plasma mass spectrometry with a 74Se-77Se double spike. Chinese J Anal Chem 36:1385–1390. doi: 10.1016/S1872-2040(08)60075-4

Appendix

Selenium typically has a low concentration in natural systems, on the order of parts per trillion (Johnson et al. 1999; Lenz and Lens 2009). As a result, selenium needs to be enriched in the samples before measurement, and have its signal intensity boosted through hydride generation (Zhu et al. 2008). Both methods have the added benefit of removing elements that interfere with selenium (Table 1). Pre-concentration techniques using thiol cotton fiber (TCF) cause little fractionation due to minimal loss of selenium on the resin (Elwaer and Hintelmann 2008a; Rouxel et al. 2002). Hydride generation can result in some fractionation of the sample, so a double spike technique was used at the beginning of sample preparation to remove any induced mass bias (Elwaer and Hintelmann 2008a).

Samples were purified using thiol cotton fiber (TCF), made using a combination of methods from Rouxel et al. (2002) and Elwaer and Hintelmann's (2008) for thiol cellulose powder, a similar material using microcrystalline cotton, rather than clean cotton balls or rolls. To make the TCF, 20 g of clean, absorbent cotton balls (Dukal Corp) were weighed into a 500 mL acid washed Teflon bottle. Then, 125 mL of 98% thioglycollic acid (Mercaptoacetic acid, Acros Organics), 70 mL acetic anhydride (Fisher Chemical), 40 mL glacial acetic acid (Fisher Chemical), 0.7 mL of 96% trace metal grade sulfuric acid (Fisher Chemical), and finally, 5 mL of MilliQ distilled water (DI) were slowly added, in order. Not all procedures for TCF include the addition of DI, but an additional volume of liquid helps saturate the cotton balls, allowing for a more homogeneous reaction. The solution was left to cool for half an hour, then was capped and shaken for 30 minutes. The bottle was

placed in a 60˚C water bath for a day, before it was removed, and shaken again for an additional 30 minutes. After another 24 hours in the hot water bath, the solution was ready to be vacuum filtered. Gently stirring the solution while rinsing the filtrate with MilliQ increases the rate of filtration. Air was pulled through the rinsed fibers using the vacuum filtration apparatus for several minutes before the finished TCF was finally scraped off the filter paper and allowed to air-dry at room temperature for a few days prior to use. The prepared TCF is stable for at least one year (Yu et al. 2001).

To pre-concentrate the samples, 0.10 g of TCF was loaded into a 1 mL polyethylene column with 0.45 μm porous frits, rinsed with 2mL of MilliQ, then packed down to remove air space using a clean, designated frit inserter. The column was then conditioned by running through an additional 2mL of MilliQ DI, 1mL of 6 N HCl, followed by 1mL of 1N HCl.

The sample must be reduced to Se(IV) before it can be processed, as Se(VI) will not sorb to the TCF. The rate of reduction is dependent on the concentration of HCl (Brimmer et al. 1987), though samples with high concentrations of Se will also take longer to completely reduce. Bye and Lund (1988) calculated the length of time needed to reduce a set percentage of the selenium based on both the temperature and the concentration of HCl.

Samples were first spiked with a 77-74 Se mixture in a 50:50 spike to sample ratio. The sample then has sufficient concentrated HCl added to bring the resulting HCl concentration to at least 4M. It was then heated in a 100˚C water bath for 25 mins, after which it was diluted to 1M HCl. If the concentration of HCl is 8M or

greater, leaving the sample at room temperature for 4 hrs was sufficient to reduce it completely. Samples must be loosely capped when heated, to prevent selenium loss. For small volume samples (< 1 mL even with acid), extra acid and time was required for reduction. Generally, adding enough concentrated HCl to reach a volume of 1mL, letting the samples reduce overnight, and diluting the samples to 1 N HCl 30 mins before processing worked adequately well.

The sample was then loaded on to the column, using enough volume to sorb 1.2 μg of Se(IV) onto the TCF. Follow with 2 mL of MilliQ, 2 mL of 6 N HCl, and finally 2 mL of 1 N HCl to dislodge any remaining interfering elements. Draw air through the column for several minutes to remove as much liquid as possible.

The TCF was popped out of the column into a 15 mL test tube and 50 μL of concentrated HNO_3 was added. The test tubes were placed in an 80˚C water bath for 20 mins, with the caps loosely attached. After heating, 2.5 mL of MilliQ is added to each, and were well shaken. The samples were then centrifuged at 5000 RPM for 5 mins, so that the liquid containing the extracted Se can be decanted into another container. Another 50 μL of HNO_3 was then added to each test tube, and the water bath and centrifuge steps repeated. The liquid was decanted into the same container previously used for each sample. The samples were filtered (0.45 μm, Acrodisc, Pall, UK), and 2.5 mL of 12 N HCl was added. The samples could then be placed into the boiling water bath for 30 min to reduce the Se(VI) back to Se(IV). The samples were then diluted to a 15 mL sample volume using MilliQ water. Samples must be left to sit overnight to equilibrate with atmospheric Kr (Schilling et al. 2011a), and must be

used shortly after purification to preserve their integrity (Conde and Sanz Alaejos 1997).

To correct for both instrumental mass bias and any fractionation caused by the separation or reduction processes, a double spike is used. Se-74 and Se-77 (ISOFLEX) were the chosen spikes, based on error propagation calculations from the double spike toolbox (Rudge et al. 2009). These same isotopes have been used as spikes in more recent research (Mitchell et al. 2012; Schilling and Wilcke 2010; Zhu et al. 2008) in place of the original Se-82 Se-74 spike (Johnson et al. 1999).

Each spike was dissolved separately in 2.5mL of concentrated Omnitrace Ultra nitric acid, and then diluted to a total volume of 500mL using 1N HCl (Omnitrace Ultra). The original mass of selenium used was too small to measure to the degree of accuracy required, so the concentration of each solution was found using an inductively coupled plasma optical emission spectrometer (ICP-OES; ICAP). Using the double spike toolbox (Rudge et al. 2009) as a guideline, the two spikes were mixed in a molar ratio of 53% Se-74 to 47% Se-77. The same toolbox was used to set a goal sample/spike ratio of 55% to 45% by concentration, as other studies have also found that the accuracy is not greatly affected if the mixture varies by 5% in either direction (Zhu et al. 2008).

Isotope ratios were measured using a Neptune MC-ICP-MS (Thermo instruments), with an APEX hydride generator (formerly known as LI-2) as the sample introduction system. A 0.2% sodium hydroxide, 0.4% sodium borohydride solution was used as the reducing reagent. Samples were in a 2N HCl matrix. Higher concentrations of HCl were originally used, but led to stability issues. All blanks

must be processed through the TCF, but do not require the reduction step. A 4N HCl solution was used to rinse between samples and blanks. An integration time of 2s was used, so that a 300-cycle measurement was approximately 10 minutes.

Data reduction was performed using an iterative set of equations based on those used by Siebert et al. (2001). The double spike inversion program can iterate any given parameter until it converges for the given set of conditions, separating the sample from the spike, and calculating the necessary ratios and delta values.

After calculating the instrumental fractionation, the isotopes were corrected for interferences from argon dimers, germanium, krypton, and any relevant hydrides. Blank corrections were performed before the initial calculations, and were usually enough to remove interferences from argon chloride, nickel oxide, krypton, and germanium and arsenic hydrides. The 83 signal was still monitored in blanks to make certain krypton is not variable enough to require additional correction.

6.1 $$\delta^{\frac{82}{78}}Se = \left(\frac{^{\frac{82}{78}}Se_{sample} - ^{\frac{82}{78}}Se_{standard}}{^{\frac{82}{78}}Se_{standard}} \right) \times 10^3‰$$

6.2 $$^{80}Se_{calc} = \left(^{78}I - ^{78}Blank\right)\left(\frac{^{80}Se_{IUPAC}}{^{78}Se_{IUPAC}}\right)\left(\frac{^{78}Se_{mass}}{^{80}Se_{mass}}\right)^{fIns}$$

6.3 $$(^{40}Ar_2^+)_{calc} = ^{80}I - ^{80}Se_{calc}$$

6.4 $$^{78}Se = ^{78}I - (^{38}Ar^{40}Ar/^{40}Ar_2)(^{40}Ar_2^+)_{calc}$$

6.5 $$^{76}Se = ^{76}I - (\left[^{38}Ar_2 + ^{36}Ar^{40}Ar\right]/^{40}Ar_2)(^{40}Ar_2^+)_{calc}$$

Where the value for the argon ratios come from the natural abundances. ^{76}Se, ^{78}Se, and ^{82}Se cannot simply be blank corrected for the final ratios, as the intensities measured in the blanks do not accurately reflect the variability of the argon

interference (Schilling and Wilcke 2010). The estimate for ^{80}Se is repeated once a corrected value of ^{78}Se is obtained. The actual quantity of argon dimer in each sample can then be obtained by iteration.

6.6 $$(^{40}Ar_2^+)_{calc} = {}^{80}I - {}^{80}Se_{calc} - {}^{83}Kr\left(\frac{^{80}Kr_{IUPAC}}{^{83}Kr_{IUPAC}}\right)\left(\frac{^{83}Kr_{mass}}{^{80}Kr_{mass}}\right)^{fIns}$$

6.7 $$^{82}Se = {}^{82}I - {}^{83}Kr\left(\frac{^{82}Kr_{IUPAC}}{^{83}Kr_{IUPAC}}\right)\left(\frac{^{83}Kr_{mass}}{^{82}Kr_{mass}}\right)^{fIns}$$

Equations used to correct for the krypton interference, if required. Levels of Kr are usually fairly low in the Ar gas supply, but the amount of Kr present does increase when the Ar tanks are almost empty. Samples are equilibrated with atmospheric Kr overnight before they are measured (Schilling et al. 2011a). Because the samples will have selenium hydride on the 83 signal, the Kr level is taken from the blank. Blank measurements are taken frequently, and Kr levels are usually sufficiently low that using the value from the blanks is sufficient.

^{82}Se has an additional interference from sulfur oxide (SO_3). The S interference is problematic, as processing the sample with thiol cotton fiber (TCF) to remove most other interfering elements adds approximately 100 mg/L of S. The SO_3 interference can be corrected by insuring that the blank is matrix matched.

6.8 $$^{74}Se = {}^{74}I - \left(^{73}Ge\right)\left(\frac{^{74}Ge_{IUPAC}}{^{73}Ge_{IUPAC}}\right)\left(\frac{^{73}Ge_{mass}}{^{74}Ge_{mass}}\right)^{fIns}$$

6.9 $$^{76}Se = {}^{76}I_{corrected\ for\ Ar} - \left(^{73}Ge\right)\left(\frac{^{76}Ge_{IUPAC}}{^{73}Ge_{IUPAC}}\right)\left(\frac{^{73}Ge_{mass}}{^{76}Ge_{mass}}\right)^{fIns}$$

The ^{74}Se signal was blank corrected for a minor Cl interference, as well as any Ge from the hydride generator or reagents. If the Ge signal was larger in the blank

than in the sample, only the blank correction on ^{74}Se was applied. ^{76}Se was also corrected for Ge.

6.10 $$^{82}SeH^{+} = {}^{83}I - {}^{83}Blank$$

6.11 $$^{77}Se = {}^{77}I - {}^{76}Se\left(\frac{^{82}SeH^{+}}{^{82}Se}\right)$$

6.12 $$^{78}Se = {}^{78}I_{corrected\ for\ Ar} - {}^{77}Se\left(\frac{^{82}SeH^{+}}{^{82}Se}\right)$$

Because H was being introduced into the system, some of the Se will exist as SeH^{+}. It then interferes with any mass that is heavier by one. Thus, a correction must be applied to ^{77}Se using ^{76}Se, and to ^{78}Se using ^{77}Se. The amount of each hydride that is produced for each isotope of Se is assumed to be equivalent to the ratio of the ^{82}Se hydride to the amount of ^{82}Se. If there is enough hydrogen and argon in the system, there can also be an $^{1}H_2{}^{40}Ar_2{}^{+}$ interference on 82, but it can be rectified via blank correction.

If there is any As in the sample, that will also produce a hydride that interferes with ^{76}Se. However, as long as the concentration of As is less than 10 times the concentration of Se, the interference can be ignored (Elwaer and Hintelmann 2007). Sufficient As is removed during the sample purification process that a correction was not required. The 75 signal is still monitored to detect whether there is any As present, but it should be noted that this signal monitors not only As, but also an Ar Cl interference ($^{40}Ar^{35}Cl$), and both $^{74}SeH^{+}$ and $^{74}GeH^{+}$. The Cl_2 and GeH^{+} interference can both be corrected using a matrix-matched blank, assuming the samples do not contain additional Ge, but the SeH^{+} corrections must be performed mathematically.